New Results on the Thermodynamic Properties of the Climate System

Valerio Lucarini

Meteorologisches Institut, Klimacampus, University of Hamburg, Hamburg, Germany, and Department of Mathematics and Statistics, University of Reading, Reading, United Kingdom

Klaus Fraedrich and Francesco Ragone

Meteorologisches Institut, Klimacampus, University of Hamburg, Hamburg, Germany

ABSTRACT

In this paper the authors exploit two equivalent formulations of the average rate of material entropy production in the climate system to propose an approximate splitting between contributions due to vertical and eminently horizontal processes. This approach is based only on 2D radiative fields at the surface and at the top of atmosphere. Using 2D fields at the top of atmosphere alone, lower bounds to the rate of material entropy production and to the intensity of the Lorenz energy cycle are derived. By introducing a measure of the efficiency of the planetary system with respect to horizontal thermodynamic processes, it is possible to gain insight into a previous intuition on the possibility of defining a baroclinic heat engine extracting work from the meridional heat flux. The approximate formula of the material entropy production is verified and used for studying the global thermodynamic properties of climate models (CMs) included in the Program for Climate Model Diagnosis and Intercomparison (PCMDI)/phase 3 of the Coupled Model Intercomparison Project (CMIP3) dataset in preindustrial climate conditions. It is found that about 90% of the material entropy production is due to vertical processes such as convection, whereas the large-scale meridional heat transport contributes to only about 10% of the total. This suggests that the traditional two-box models used for providing a minimal representation of entropy production in planetary systems are not appropriate, whereas a basic—but conceptually correct—description can be framed in terms of a four-box model. The total material entropy production is typically 55 mW m^{-2} K^{-1}, with discrepancies on the order of 5%, and CMs' baroclinic efficiencies are clustered around 0.055. The lower bounds on the intensity of the Lorenz energy cycle featured by CMs are found to be around 1.0–1.5 W m^{-2}, which implies that the derived inequality is rather stringent. When looking at the variability and covariability of the considered thermodynamic quantities, the agreement among CMs is worse, suggesting that the description of feedbacks is more uncertain. The contributions to material entropy production from vertical and horizontal processes are positively correlated, so that no compensation mechanism seems in place. Quite consistently among CMs, the variability of the efficiency of the system is a better proxy for variability of the entropy production due to horizontal processes than that of the large-scale heat flux. The possibility of providing constraints on the 3D dynamics of the fluid envelope based only on 2D observations of radiative fluxes seems promising for the observational study of planets and for testing numerical models.

1. Introduction

It has long been recognized that adopting a thermodynamic perspective, as pioneered by Lorenz (1955, 1967), may prove of great utility for providing a satisfactory theory of climate dynamics able to tackle simultaneously balances of physical quantities and dynamical instabilities, and aimed at explaining the global structural properties of the climate system, as envisaged by Saltzman (2002). This is of great relevance in terms of the pursuit for explaining climate variability and change on a large variety of scales, covering major paleoclimatic shifts and almost regularly repeated events such as ice ages, as well as ongoing and future anthropogenic climate change. Additionally, this strategy may prove of great relevance for the provision of reliable metrics for the validation of climate models (CMs), as requested by the Intergovernmental Panel on Climate Change (Solomon et al. 2007) and discussed, for example, in Held (2005)

Corresponding author address: Valerio Lucarini, Meteorologisches Institut, Klimacampus, University of Hamburg, Grindelberg 5 20144 Hamburg, Germany.
E-mail: valerio.lucarini@zmaw.de

and Lucarini (2008a). See Lucarini and Ragone (2011) for a recent example.

Along the lines of nonequilibrium macroscopic thermodynamics (Prigogine 1962; de Groot and Mazur 1984), the climate can be seen as a nonequilibrium system, which transforms potential into mechanical energy like a thermal engine and generates entropy by irreversible processes. When the external and internal parameters have fixed values, the climate system achieves a steady state by balancing the thermodynamic fluxes with the surrounding environment (Peixoto and Oort 1992).

The concept of the energy cycle of the atmosphere introduced by Lorenz (1955, 1967) allowed for defining an effective climate machine such that the atmospheric and oceanic motions simultaneously result from the mechanical work (then dissipated in a turbulent cascade) produced by the engine, and reequilibrate the energy balance of the climate system (Stone 1978a,b; Barry et al. 2002). Johnson (2000) introduced a Carnot engine–equivalent picture of the climate system by defining effective warm and cold reservoirs and their temperatures. Recently, Tailleux (2009) proposed a fresh outlook on the energetics of the ocean circulation along similar lines.

The interest in studying climate irreversibility largely stems from the proposal of the maximum entropy production principle (MEPP) by Paltridge (1975), which suggests that the climate is a nonequilibrium nonlinear systems adjusting in such a way as to maximize the entropy production (Grassl 1981; Mobbs 1982; Kleidon and Lorenz 2005; Martyushev and Seleznev 2006). Even if recent claims of ab initio derivation of MEPP (Dewar 2005) have been dismissed (Grinstein and Linsker 2007) and strong criticisms have arisen within the geophysical community (Goody 2007), this principle has stimulated the reexamination of entropy production in the climate system (Peixoto et al. 1991; Goody 2000; Fraedrich and Lunkeit 2008; Pascale et al. 2010) and the development of new strategies for improving the parameterizations of climate models (Kleidon et al. 2006). Moreover, a more detailed analysis of the various processes responsible for the entropy production has led to clarifying the relative role of contributions due to radiative processes, mainly related to the degradation of the photons exergy by the thermalization of the solar radiation at terrestrial temperatures (Wu and Liu 2009), and those due to the turbulent processes related to the motions of the fluid envelope of the planet (Goody 2000). The latter contributions, which add up to the so-called material entropy production, are expected, despite being relatively small, to be of greater relevance as diagnostics of the large-scale properties of the system (Ozawa et al. 2003; Lucarini 2009a).

In recent years, a great effort has been devoted to improving the thermodynamic description of the climate system by taking into account in a more profound way the irreversible processes associated with the mixing and phase changes of water vapor (Goody 2000; Pauluis 2000; Pauluis and Held 2002a,b; Romps 2008). While these theoretical contributions are crucial for assessing with a higher degree of precision the components of the entropy budget of the climate system, we shall see that a simpler and more manageable description of the climate thermodynamics shows excellent performance in estimating the material entropy production of the system.

We should note that when the material entropy production of the climate system is analyzed, most of the attention is devoted to atmospheric processes, with the ocean being of relevance only as a boundary condition with a role not qualitatively different from that of land surface. While being of great relevance when the energetics of the climate system is considered, the contribution to the material entropy production resulting from oceanic processes is indeed negligible (Shimokawa and Ozawa 2001), basically because, apart from the mixed layer, the ocean is up to a good approximation an isothermal fluid. The oceanic entropy production is found to be less than 2% of the atmospheric one (Pascale et al. 2010).

Recently, a link has been found among the Carnot efficiency, the intensity of the Lorenz energy cycle, the material entropy production, and the degree of irreversibility of the climate system (Lucarini 2009a)—namely, the efficiency of the equivalent thermal machine sets also the proportionality between the internal entropy fluctuation of the system and the lower bound to entropy production by the fluid compatible with the second law of thermodynamics. Such a bound is basically given by the entropy produced by the dissipation of the mechanical energy, whereas the excess of entropy production is due to the turbulent transport of heat down the gradient the temperature field.

These results have paved the way for a new, extensive exploration aimed at understanding the climate response under various scenarios of forcings, of atmospheric composition, and of boundary conditions. Recent preliminary efforts using the Planet Simulator model (PLASIM) (Fraedrich et al. 2005), a simplified yet earth-like climate model, have focused on the impacts on the thermodynamics of the climate system of changes in the solar constant, with an analysis of the onset and decay of snowball earth conditions (Lucarini et al. 2010a), and on those due to changing CO_2 concentration (Lucarini et al. 2010b).

When performing a complete thermodynamic analysis of the planetary system, a potentially serious problem

is that three-dimensional, time-dependent information about the intensive thermodynamic quantities, their tendencies, and the forcing terms is required (Lucarini 2009a). It has been proven that for a given numerical model constructing the suitable diagnostic tools is feasible and definitely not computationally burdensome, as only integral operators (which boil down to weighted sums) are involved (Fraedrich and Lunkeit 2008). On the other side, deducing the thermodynamics of the system from observations is a rather complex matter, since it is hard to obtain accurate reconstructions of all the involved 3D thermodynamic quantities with sufficient spatial and temporal resolution. Such a problem arises also when an intercomparison analysis covering a large number of CMs is pursued, because the needed climate fields are not necessarily among those routinely provided for public download, as discussed by Lucarini and Ragone (2011).

In this paper we introduce an approximate formula that allows for splitting the material entropy production into two contributions, one related to horizontal, planetary-scale transport processes and the other related to vertical processes. The two contributions can be computed separately using 2D radiative fields at the top of the atmosphere (TOA) and at the surface. The contribution to the material entropy production due to horizontal processes can be computed using 2D radiative fields at the top of the atmosphere only. Such estimation allows for computing a lower bound to the total values of material entropy production and intensity of the Lorenz energy cycle, or, equivalently, of the average rate of total dissipation of the kinetic energy. Moreover, by combining energy and entropy constraints, it is possible to gain insight into a previous intuition as to the possibility of defining a baroclinic heat engine extracting work from the meridional heat flux (Barry et al. 2002). We take advantage of our approach to analyze the thermodynamic properties of the preindustrial (PI) control runs of the CMs included in the Program for Climate Model Diagnosis and Intercomparison (PCMDI)/phase three of the Coupled Model Intercomparison Project (CMIP3) dataset, thus extending the results of Lucarini and Ragone (2011) to the "second law of thermodynamics" diagnostics. We take into account first and second moments of thermodynamic quantities describing out-of-equilibrium properties, in order to assess their climatology and their (co)variability, thus testing equilibration processes.

The paper is divided as follows. In section 2 we review two distinct formulas allowing for evaluating the material entropy production of a generic planetary system and perform a suitable scale analysis, obtaining simplified expressions making use of 2D fields at the surface and TOA only. In section 3 we show how to derive from the above described approximate formulas general bounds on the material entropy production and on the degree of irreversibility of the system. We also clarify the basic features required in simplified box models (see, e.g., Kleidon and Lorenz 2005) for describing the fundamental properties of entropy production in the earth system. In section 4 we verify the validity of the approximate formula and exploit it to estimate the thermodynamic properties of the CMs included in the PCMDI/CMIP3 dataset in preindustrial climate conditions. In section 5 we present our conclusions and perspectives for future work. An appendix is devoted to clarifying a crucial estimate used in the paper.

2. Rate of material entropy production

a. Theoretical outlook

The traditional approach for the investigation of the entropy production of the climate system relies on separating the contributions due to irreversible processes involving matter and those due to irreversible changes in the spectral properties of the radiation.

The process of thermalization of the solar radiation gives by far the most important contribution to the global planetary entropy production, basically because it involves the transformation of electromagnetic energy traveling through space obeying a Planckian spectrum with the temperature signature of the sun's corona (about 5800 K) into (quantitatively identical) electromagnetic energy whose spectral properties are approximately described by a Planckian spectrum at the earth's emission temperature (about 250 K). A very detailed and extensive account of these processes and their contribution in terms of entropy production has recently been given by Wu and Liu (2009).

The rest of the irreversible processes taking place in the climate system provide a much smaller contribution to the entropy production, basically because much less relevant temperature (or chemical potential) differences are involved. The irreversible transformations occurring in the climate system involve in principle a great variety of phenomena, including dissipation of mechanical energy, heat transport down the temperature gradient, irreversible mixing, and phase transitions.

In a system at steady state, the expectation value of the extensive, integrated material entropy does not depend on time. Following Johnson (2000) and Goody (2000), it is possible to derive the following equation for the total entropy S of the climate system:

$$\overline{\dot{S}} = \int_{\Omega} \left(\overline{\frac{\dot{q}_{\text{rad}}}{T}} + \overline{\dot{s}_{\text{turb}}} \right) dV = 0, \qquad (1)$$

where Ω is the spatial domain of integration, the dot indicates the operation of time derivative, the overbar indicates the operation of long-term average, T is the local temperature of the medium, $\dot{q}_{rad}$ is the heating due to the convergence of the radiation fluxes, and $\dot{s}_{turb}$ is the density of entropy production due to irreversible processes involving the fluid medium, usually referred to as local material entropy production (Ozawa et al. 2003). Therefore, we obtain

$$\overline{\dot{S}_{mat}} = \int_{\Omega} \overline{\dot{s}_{turb}}\ dV = -\int_{\Omega} \overline{\frac{\dot{q}_{rad}}{T}}\ dV, \qquad (2)$$

where $\overline{\dot{S}_{mat}}$ is the average rate of material entropy production of the climate system. This equation provides us with two recipes for computing the material entropy production, one based on the direct computation of the spatial integral of $\dot{s}_{turb}$ and the other (the "inverse formula") based on the evaluation of the interaction between radiation and matter. Depending on the degree of detail and precision we adopt in the representation of the physicochemical properties of the climate system, we may derive different expressions for $\dot{s}_{turb}$ that are suited for characterizing a wider or smaller number of irreversible processes.

Commonly, the following expression is adopted for the computation of the material entropy production budget:

$$\dot{s}_{turb} = \frac{\varepsilon^2}{T} + F_{SH} \cdot \mathbf{\nabla}\frac{1}{T} + F_{LH} \cdot \mathbf{\nabla}\frac{1}{T}. \qquad (3)$$

In this expression, ε^2 is the dissipation of kinetic energy, which also takes into account the friction of the falling hydrometeors—there are many discussions of this rather controversial issue (see, e.g., Goody 2000; Pauluis et al. 2000; Rennó 2001; Lorenz and Rennó 2002; Kleidon and Lorenz 2005)—while F_{SH} and F_{LH} are the sensible and latent heat fluxes, respectively. Note that F_{SH} refers to a small-scale turbulent flux, while F_{LH} refers to both small-scale turbulent and large-scale fluxes, the large-scale transport of water vapor being an important component of the global entropy production budget. The hydrological cycle is indeed a key element of the thermodynamics of the climate system. Such a formula has been widely used for estimating the entropy production of the earth system (Peixoto et al. 1991; Peixoto and Oort 1992; Fraedrich and Lunkeit 2008; Pascale et al. 2010; Lucarini et al. 2010a,b)

Romps (2008) refers to the representation of the entropy production given by Eq. (3) as resulting from the bulk heating budget because water is treated mainly as a passive substance, while processes such as irreversible mixing of the water vapor are altogether ignored. More detailed descriptions of the "moist" atmosphere have led to formulations of atmospheric thermodynamics able to account for these processes (Goody 2000; Pauluis 2000; Pauluis and Held 2002a,b; Romps 2008). Moreover, additional contributions to the entropy production are given by the irreversible mixing of salt in the ocean (Shimokawa and Ozawa 2001). Such more refined formulations of the entropy processes inside the climate system account for a consistent treatment of the entropy generated by the hydrological cycle. Given the complex nature of the climate system, additional processes contributing to entropy production can be highlighted. Kleidon (2009) presents a complete and holistic account of this issue, suggesting that biological and geochemical processes, as well as the great variety of chemical processes taking place in the atmosphere, should in principle be included to get a truly complete treatment of the entropy budget of the earth system. None of these processes is usually explicitly represented in current climate models.

Since we aim at a parsimonious but efficient representation of the entropy production of the climate system, we would like to be able to choose an approach that translates into an explicit expression for $\dot{s}_{turb}$, which is as simple as possible but at the same time provides a good approximation to the entropy production. Moreover, when using our formula to compute the entropy production using data from a numerical model, it makes no sense to take into account processes that are not represented in the model. One should also note that the entropy production due to unphysical processes present in the model (numerical diffusion, dispersion, etc.) should be in principle taken into account if accurate calculations are sought after. Previous analyses of the detailed budget of entropy production in climate models have shown that these contributions are, fortunately, almost negligible when the total entropy production is considered, unlike the various contributions coming from the various involved irreversible physical processes (Pascale et al. 2010; see below).

On the other hand, the time average of the volume integration of $-\dot{q}_{rad}/T$ gives the exact value of the entropy production, so that the indirect approach allows us on one hand to obtain precise estimates, and on the other to test the validity of different explicit formulations for $\dot{s}_{turb}$ and, consequently, of the level of detail we adopt in describing the climatic thermodynamic processes.

Interpreting previous climate models' results is definitely useful in this direction. Pascale et al. (2010), who considered two fully coupled atmosphere–ocean climate models, clearly showed that in present-day conditions the identity given by Eq. (2) is obeyed up to an excellent

degree of precision when we use for $\dot{s}_{\text{turb}}$ the expression given in Eq. (3). The observed agreement is within 1% and of the same order of magnitude of the uncertainty in the material entropy production due to the bias in the imperfect closure of the energy cycle related to spurious energy sinks/sources inside the system (Lucarini et al. 2010a,b; Lucarini and Ragone 2011). We may then conclude that whereas the sophisticated thermodynamic framework developed in Pauluis (2000), Pauluis and Held (2002a,b), and Romps (2008) is crucial for understanding in detail the various terms contributing to the entropy budget of the climate system, the simpler formulation given in Eq. (3) (Peixoto et al. 1991; Peixoto and Oort 1992; Fraedrich and Lunkeit 2008; Pascale et al. 2010; Lucarini et al. 2010a,b) provides rather accurate results when only the material entropy production is taken into account. Note that Goody (2000) observed that adopting a more detailed physical description of the atmosphere where irreversible water vapor mixing processes are considered changes only slightly the estimate of the material entropy production. He attributed this to a spurious coincidence, but given the

results of Pascale et al. (2010), it is far more likely that treating the latent heat release and absorption in a simplified way boils down to adding up the most important contributions composing the detailed entropy budget advocated in Pauluis (2000), Pauluis and Held (2002a,b), and Romps (2008).

It should also be noted that the overall contribution of the subsurface oceanic processes to the entropy production of the climate system is negligible, the basic reason being that to a good approximation the deep ocean is an isothermal fluid, so that heat transport generates little entropy (Pascale et al. 2010). From now on, we consider entropy generation as a matter involving only processes in the atmosphere and processes entailing energy exchanges between the atmosphere and the underlying surface, which can correspond to either land or ocean.

b. Scale analysis: Direct expression of entropy production

The "direct" expression for the material entropy production is considered first. Using Gauss' theorem, we can write

$$
\overline{\dot{S}_{\text{mat}}} = \int_{\Omega} \overline{\frac{\varepsilon^2}{T}} \, dV + \int_{\Omega} \overline{\mathbf{F} \cdot \mathbf{\nabla}\frac{1}{T}} \, dV = \int_{\Omega} \overline{\frac{\varepsilon^2}{T}} \, dV + \int_{\Omega} \overline{\mathbf{\nabla} \cdot \left(\frac{\mathbf{F}}{T}\right)} \, dV - \int_{\Omega} \overline{\left(\frac{\mathbf{\nabla} \cdot \mathbf{F}}{T}\right)} \, dV
$$

$$
= \int_{\Omega} \overline{\frac{\varepsilon^2}{T}} \, dV + \int_{\partial\Omega} \overline{\hat{n} \cdot \left(\frac{\mathbf{F}}{T}\right)} \, dA - \int_{\Omega} \overline{\left(\frac{\mathbf{\nabla} \cdot \mathbf{F}}{T}\right)} \, dV = \int_{\Omega} \overline{\frac{\varepsilon^2}{T}} \, dV - \int_{\Omega} \overline{\left(\frac{\mathbf{\nabla} \cdot \mathbf{F}}{T}\right)} \, dV, \tag{4}
$$

where $\partial\Omega$ refers to the boundary of the domain Ω. As discussed in Lucarini (2009a), the volume integral of the first term on the right-hand side of Eq. (4) basically gives us the lower bound to the entropy production compatible with the system having a global mean dissipation of kinetic energy (and production of mechanical work) equal to $\overline{W} = \overline{D} = \int \overline{\varepsilon^2} \, dV$. The second term in Eq. (4) vanishes as no material fluxes are present at the top of the atmosphere. The material flux $\mathbf{F}$ accounts for both the sensible and latent heat fluxes, so that $\mathbf{F} = F_{\text{SH}} + F_{\text{LH}}$. The two fluxes have rather different properties since sensible heat turbulent transport is mostly relevant for the interaction between the surface and the boundary layer of the atmosphere, whereas the latent heat flux is such that it picks up water vapor at unsaturated, relatively warm surface conditions and transports it to regions with lower temperatures where condensation and precipitation occur. Turbulent transport occurs mainly in the vertical direction (Peixoto and Oort 1992), so that $\mathbf{\nabla} \cdot F_{\text{SH}} \approx \partial_z F_z^{\text{SH}}$. In the case of latent heat, this approximation does not hold, since the large-scale horizontal transport is an important component of F_{LH}.

Nevertheless, extending the approach by Fraedrich and Lunkeit (2008), we can rewrite Eq. (4) in a simpler 2D form as

$$
\overline{\dot{S}_{\text{mat}}} = \overline{\dot{S}_{\text{mat}}^{\text{diss}}} + \overline{\dot{S}_{\text{mat}}^{\text{SH}}} + \overline{\dot{S}_{\text{mat}}^{\text{LH}}}
$$

$$
= \int_A \overline{\frac{\langle\varepsilon^2\rangle}{T_{\text{diss}}}} \, dA - \int_A \overline{F_{z,\text{surf}}^{\text{SH}}\left(\frac{1}{T_{\text{SH}}^+} - \frac{1}{T_{\text{SH}}^-}\right)} \, dA
$$

$$
- \int_A \overline{F_{z,\text{surf}}^{\text{LH}}\left(\frac{1}{T_{\text{LH}}^+} - \frac{1}{T_{\text{LH}}^-}\right)} \, dA + \Delta\overline{\dot{S}_{\text{mat}}^{\text{LH}}}, \tag{5}
$$

where A spans over the horizontal extent of the atmosphere; $\overline{\dot{S}_{\text{mat}}^{\text{diss}}}$, $\overline{\dot{S}_{\text{mat}}^{\text{SH}}}$, and $\overline{\dot{S}_{\text{mat}}^{\text{LH}}}$ are respectively the contributions to the material entropy production due to energy dissipation and sensible and latent heat fluxes; $\langle\varepsilon^2\rangle = \int \varepsilon^2 \, dz$ is the vertically integrated dissipational heating; $T_{\text{diss}} = \int \overline{\varepsilon^2} \, dz / \int \overline{\varepsilon^2/T} \, dz$ is a suitably time averaged 2D field of characteristic temperature for energy dissipation; $\overline{F_{z,\text{surf}}^{\text{SH}}}$ and $\overline{F_{z,\text{surf}}^{\text{LH}}}$ are the long-term averages of the vertical components of sensible and latent heat fluxes at the surface (positive upward); T_{SH}^+, T_{LH}^+, T_{SH}^-, and T_{LH}^- are

2D fields of locally (in each column) define characteristic temperatures respectively of removal and absorption of sensible and latent heat; and $\Delta \dot{S}_{\text{mat}}^{\text{LH}}$ is a correction term whose meaning is explained in the following. Formally, this is achieved by dividing each column into two domains in the z direction, one where $\partial_z F_z$ is positive and one where $\partial_z F_z$ is negative. The two temperatures are then defined similarly to T_{diss}. Note that this operation is performed separately for the latent and sensible heat flux. As in each column most of the sensible and latent heat is removed at or very close to the surface, we assume that $T_{\text{SH}}^+ \approx T_{\text{LH}}^+ \approx T_{\text{surf}}$. Instead, we expect that T_{SH}^- is closely approximated by the temperature of the boundary layer T_{BL}, while we indicate T_{LH}^- with T_C, since it refers to the average condensation temperature. Therefore we can write

$$\overline{\dot{S}}_{\text{mat}} = \overline{\dot{S}}_{\text{mat}}^{\text{diss}} + \overline{\dot{S}}_{\text{mat}}^{\text{SH}} + \overline{\dot{S}}_{\text{mat}}^{\text{LH}}$$

$$= \int_A \frac{\langle \varepsilon^2 \rangle}{T_{\text{diss}}} dA - \int_A \overline{F_{z,\text{surf}}^{\text{SH}}} \left(\frac{1}{T_{\text{surf}}} - \frac{1}{T_{\text{BL}}} \right) dA$$

$$- \int_A \overline{F_{z,\text{surf}}^{\text{LH}}} \left(\frac{1}{T_{\text{surf}}} - \frac{1}{T_C} \right) dA + \Delta \overline{\dot{S}}_{\text{mat}}^{\text{LH}}. \qquad (6)$$

Let us now see how the correction term $\Delta \overline{\dot{S}}_{\text{mat}}^{\text{LH}}$ arises. In the case of the latent heat, because of the presence of horizontal large-scale transports of moisture, it is not possible to define rigorously the condensation temperatures locally in each column, since not all the moisture that evaporates at the bottom of a certain atmospheric column will condense right above but will partly be transported horizontally outside of the column. In present-day climate moisture is transported from the tropical regions between 10° and 40°N/S to the equatorial region and to the middle and high latitudes, fuelling respectively the deep convection in the uplifting branch of the Hadley cell and the baroclinic processes of the midlatitudes (see, e.g., Table 7.1 in Peixoto and Oort 1992). We can write the latent heat due to surface evaporation as $\overline{F_{z,\text{surf}}^{\text{LH}}} = \overline{F_{\text{loc}}^{\text{LH}}} + \overline{F_{\text{out}}^{\text{LH}}}$, where $\overline{F_{\text{loc}}^{\text{LH}}}$ and $\overline{F_{\text{out}}^{\text{LH}}}$ are the latent heat fluxes related respectively to the part of water vapor that condenses at T_C in the same column where it is evaporated, and to the part that is transported and condensed somewhere else at the effective condensation temperature T_C'. Therefore, the correct expression for the material entropy production for an atmospheric column related to the water phase changes is (neglecting contributions from reevaporation of falling rain droplets)

$$- \overline{F_{\text{loc}}^{\text{LH}}} \left(\frac{1}{T_{\text{surf}}} - \frac{1}{T_C} \right) - \overline{F_{\text{out}}^{\text{LH}}} \left(\frac{1}{T_{\text{surf}}} - \frac{1}{T_C'} \right). \qquad (7)$$

We can rewrite the expression given in Eq. (7) as

$$- (\overline{F_{\text{loc}}^{\text{LH}}} + \overline{F_{\text{out}}^{\text{LH}}}) \left(\frac{1}{T_{\text{surf}}} - \frac{1}{T_C} \right) - \overline{F_{\text{out}}^{\text{LH}}} \left(\frac{1}{T_C} - \frac{1}{T_C'} \right)$$

$$= - \overline{F_{z,\text{surf}}^{\text{LH}}} \left(\frac{1}{T_{\text{surf}}} - \frac{1}{T_C} \right) + \Delta \overline{\dot{s}_{\text{mat}}^{\text{LH}}}, \qquad (8)$$

where

$$\Delta \overline{\dot{s}_{\text{mat}}^{\text{LH}}} = - \overline{F_{\text{out}}^{\text{LH}}} \left(\frac{1}{T_C} - \frac{1}{T_C'} \right) \qquad (9)$$

is the correction term due to the fact that part of the moisture that evaporates at a certain location is transported and condensed elsewhere. If T_C' is higher than T_C, we have a negative correction term (e.g., moisture transport from the tropics to the equator); otherwise, it is positive (e.g., moisture transport from the tropics to the midlatitudes). The surface integral of the term given in Eq. (9) gives exactly $\Delta \dot{S}_{\text{mat}}^{\text{LH}}$. It is possible to show that $\Delta \dot{S}_{\text{mat}}^{\text{LH}}$ is rather small, since we can prove that its absolute value is less than 5×10^{-3} W m^{-2} K^{-1}, one order of magnitude less than the value for $\dot{S}_{\text{mat}}^{\text{LH}}$ computed by Pascale et al. (2010). We present a detailed derivation of this result in the appendix.

Since the turbulent transport of sensible heat is an eminently local process, its contribution $\overline{\dot{S}}_{\text{mat}}^{\text{SH}}$ to the material entropy production is not very large. Instead, the contribution to the material entropy production coming from latent heat $\overline{\dot{S}}_{\text{mat}}^{\text{LH}}$ is largely dominant and involves evaporation, condensation, and transport processes occurring in the context of the hydrological cycle (see also Pascale et al. 2010).

Note that it is possible to define the degree of irreversibility of the system (Lucarini 2009a) by introducing the parameter $\alpha = (\overline{\dot{S}}_{\text{mat}}^{\text{SH}} + \overline{\dot{S}}_{\text{mat}}^{\text{LH}}) / \overline{\dot{S}}_{\text{mat}}^{\text{diss}}$, where symbols refer to Eq. (5). When $\alpha = 0$ the system features the smallest rate of material entropy production compatible with the presence of a Lorenz energy cycle of intensity $\overline{W} = \overline{D} = \int \overline{\varepsilon^2} dV$. If $\alpha = 0$, all the entropy is generated via dissipation of kinetic energy, with no contributions coming from fluxes transporting heat down the gradient of the temperature. Recent model simulations have shown that warmer climate conditions trigger a fast increase in the degree of irreversibility of the earth system, the main reason being the large sensitivity of latent heat fluxes to increases in the atmospheric and surface temperature (Lucarini et al. 2010a,b).

c. Scale analysis: Indirect expression of entropy production

The "indirect" expression for the material entropy production is considered now. We emphasize that such an approach bypasses the problems related to the details

in the representation of the atmospheric processes discussed at the beginning of this section. The solar short-wave (SW) radiation heats the system, whereas the infrared longwave (LW) radiation acts as a net cooler. Moreover, we split processes occurring within the atmosphere from those occurring at surface, which we interpret as boundary between the gaseous medium and the solid and liquid medium, thus moving along the lines of the *net exchange formulation* (Green 1967). Along the same lines followed to derive Eq. (5), we write the average rate of material entropy production as follows:

$$
\overline{\dot{S}_{\mathrm{mat}}} = \int_A \frac{\overline{F_{z,\mathrm{surf}}^{\mathrm{SW}}} + \overline{F_{z,\mathrm{surf}}^{\mathrm{LW}}}}{T_{\mathrm{surf}}} \, dA + \int_A \frac{\overline{F_{z,\mathrm{TOA}}^{\mathrm{SW}}} - \overline{F_{z,\mathrm{surf}}^{\mathrm{SW}}}}{T_{A,\mathrm{SW}}} \, dA
$$
$$
+ \int_A \frac{\overline{F_{z,\mathrm{TOA}}^{\mathrm{LW}}} - \overline{F_{z,\mathrm{surf}}^{\mathrm{LW}}}}{T_{A,\mathrm{LW}}} \, dA, \tag{10}
$$

where $\overline{F_{z,\mathrm{surf}}^{\mathrm{SW}}}$ and $\overline{F_{z,\mathrm{surf}}^{\mathrm{LW}}}$ are the average vertical fluxes of SW and LW radiation at surface, while $\overline{F_{z,\mathrm{TOA}}^{\mathrm{SW}}}$ and $\overline{F_{z,\mathrm{TOA}}^{\mathrm{LW}}}$ are the average vertical fluxes of SW and LW radiation at the top of the atmosphere. All the vertical fluxes are considered to be positive upward, as for the sensible and latent heat fluxes in the previous subsection. Similarly to the discussion in the previous subsection, $T_{A,\mathrm{SW}}$ and $T_{A,\mathrm{LW}}$ represent the 2D fields of characteristic atmospheric temperatures at which the interactions between matter and SW and LW radiation, respectively, occur. On our planet, most of the SW radiation is absorbed at surface or in the first few meters of ocean, so that the atmosphere is heated from below. We may rewrite Eq. (10) as follows:

$$
\overline{\dot{S}_{\mathrm{mat}}} = \int_A \overline{F_{z,\mathrm{surf}}^{\mathrm{SW}}} \left(\frac{1}{T_{\mathrm{surf}}} - \frac{1}{T_{A,\mathrm{SW}}} \right) dA
$$
$$
+ \int_A \overline{F_{z,\mathrm{surf}}^{\mathrm{LW}}} \left(\frac{1}{T_{\mathrm{surf}}} - \frac{1}{T_{A,\mathrm{LW}}} \right) dA
$$
$$
+ \int_A \frac{\overline{F_{z,\mathrm{TOA}}^{\mathrm{SW}}}}{T_{A,\mathrm{SW}}} \, dA + \int_A \frac{\overline{F_{z,\mathrm{TOA}}^{\mathrm{LW}}}}{T_{A,\mathrm{LW}}} \, dA. \tag{11}
$$

We now assume as an ansatz that $T_{A,\mathrm{SW}} \approx T_{A,\mathrm{LW}} \approx T_E = \sqrt[4]{\overline{F_{z,\mathrm{TOA}}^{\mathrm{LW}}}/\sigma}$, where T_E is the 2D field of the emission temperature of the planet (σ is the Stefan–Boltzmann constant). This means that the vertically averaged characteristic temperature of *atmospheric* absorption and emission are similar. This is the crucial approximation of our approach, motivated by the fact that most of the shortwave absorption in the atmosphere is due to water vapor (Kiehl and Trenberth 1997), which plays a major role also in determining the absorption and emission of longwave radiation in the troposphere. The contribution to shortwave radiation absorption of water vapor is about 3 times as much as that of O_3. This approximation is supported by the estimates presented by Fraedrich and Lunkeit (2008); its validity will be investigated in more quantitative terms in a future publication. For the purposes of the present paper, the approximation will be tested by comparing the values obtained with Eq. (12) with "exact" values obtained from the direct expression, in the case of the third climate configuration of the Met Office Unified Model (HadCM3) general circulation model analyzed in Pascale et al. (2010) (see section 4). We then obtain

$$
\overline{\dot{S}_{\mathrm{mat}}} \approx \int_A (\overline{F_{z,\mathrm{surf}}^{\mathrm{SW}}} + \overline{F_{z,\mathrm{surf}}^{\mathrm{LW}}}) \left(\frac{1}{T_{\mathrm{surf}}} - \frac{1}{T_E} \right) dA + \int_A \frac{\overline{F_{z,\mathrm{TOA}}^{\mathrm{SW}}} + \overline{F_{z,\mathrm{TOA}}^{\mathrm{LW}}}}{T_E} \, dA
$$
$$
\approx \int_A (\overline{F_{z,\mathrm{surf}}^{\mathrm{SW}}} + \overline{F_{z,\mathrm{surf}}^{\mathrm{LW}}}) \left(\frac{1}{T_{\mathrm{surf}}} - \frac{1}{T_E} \right) dA - \int_A \frac{\overline{\boldsymbol{\nabla_H} \cdot \overline{\mathbf{H}}}}{T_E} \, dA \approx \overline{\dot{S}_{\mathrm{mat}}^{\mathrm{vert}}} + \overline{\dot{S}_{\mathrm{mat}}^{\mathrm{hor}}}, \tag{12}
$$

where in the last passage we have used the fact that the convergence of large-scale, nonturbulent reversible enthalpy horizontal transport **H** balances the net radiative balance at the top of the atmosphere when long-term averages are considered (Peixoto and Oort 1992; Lucarini and Ragone 2011). Equation (12) tells us that the material entropy production, alternatively to the splitting proposed in Eq. (5), can be conceptually decomposed into two terms. The term $\overline{\dot{S}_{\mathrm{mat}}^{\mathrm{vert}}}$ describes the vertical transport of radiation between two reservoirs, one at the surface temperature and the other at the

temperature of the bulk of the atmosphere, and is closely related to dry and moist convective processes (Emanuel 2000). This term treats the fluid envelope as a collection of independent vertical columns dominated by fast exchanges and interactions. The term $\overline{\dot{S}_{\mathrm{mat}}^{\mathrm{hor}}}$ describes the effect of horizontally transporting energy in a 2D fluid system with spatially varying temperature structure, and is associated with longer time scales. Both terms are positive, the first because the atmosphere is on the average colder than the underlying surface, as the system is heated from below, and the second because
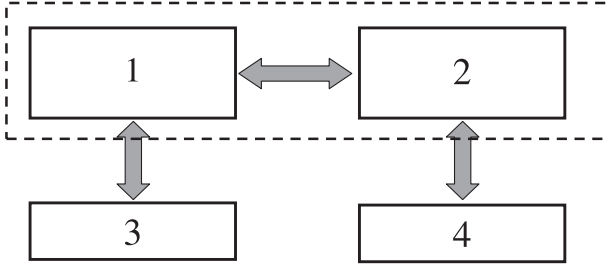
FIG. 1. Minimal conceptual diagram for the material entropy production of a planetary system as deduced from Eq. (11). Boxes 1 and 2 represent warm (low latitudes) and cold (high latitudes) fluid domains, coupled by enthalpy transport. Boxes 3 and 4 represent warm (low latitudes) and cold (high latitudes) surface domains, coupled vertically to the corresponding fluid boxes, but not to each other. The dashed rectangle encloses the reduced two-box model usually considered in previous literature.

temperature is expected to be on the average lower where there is convergence of enthalpy fluxes, and larger where divergence is observed, in agreement with the second law of thermodynamics (Peixoto and Oort 1992; Ambaum 2010). The two spatial fields whose integrals give $\dot{S}_{\mathrm{mat}}^{\mathrm{vert}}$ and $\dot{S}_{\mathrm{mat}}^{\mathrm{hor}}$ are expected to have different properties, as the former should be positive everywhere, because each column is described in the first approximation as a quasi-isolated system producing entropy, whereas the sign of the latter will depend on the sign of the radiative budget at TOA.

Note that a discretized version of the second term in Eq. (12), based on a two-box approximation of the fluid envelope of the climate system, has been considered as proxy for the total material entropy production (e.g., Lorenz et al. 2001). Instead, from Eq. (12) it is apparent that a minimal model of the whole material entropy production of a planetary system must include, in addition to the box of the warm (box 1) and cold (box 2) portions of the fluid envelope of the planet, two additional boxes, each representing the planetary surface in the warm (box 3) and cold (box 4) regions of the planet. See Fig. 1 for a conceptual scheme, where the arrows indicate the couplings defining the time evolution of the system. Note that the ocean has a dual role: on the one hand, it acts a lower surface exchanging with the atmosphere sensible and latent heat fluxes (as done by the land surface), and on the other hand it has the dynamic role of contributing, as part of the fluid envelope of the planet, to the transport of heat from the warm to the cold box. We remark again that the internal oceanic processes give only a minor contribution to the entropy production (Pascale et al. 2010).

3. Bounds to the thermodynamic properties of the climate system

We now wish to derive some bounds to the thermodynamic properties of the climate system based on only a very limited set of coarse-resolution data. Since the water vapor saturation mixing ratio strongly increases with temperature, and since on the earth the atmospheric temperature decreases with height, the vertical scale of water vapor in globally saturated conditions is smaller than that of the atmosphere. Therefore, we can assume $T_C > T_E$, as confirmed by actual estimates (Peixoto and Oort 1992; Fraedrich and Lunkeit 2008; Pascale et al. 2010). Since, as discussed above, $T_{\mathrm{BL}} \approx T_{\mathrm{surf}}$, we definitely have that $T_{\mathrm{BL}} > T_E$. Therefore, by substituting T_E for the values of the temperatures at which the latent and sensible heat are absorbed, respectively T_C and T_{BL}, for the various terms given in Eq. (5), we derive the following inequality:

$$\overline{\dot{S}_{\mathrm{mat}}} < \int_A \frac{\overline{\varepsilon^2}}{T_{\mathrm{diss}}}\, dA - \int_A (\overline{F_{z,\mathrm{surf}}^{\mathrm{SH}}} + \overline{F_{z,\mathrm{surf}}^{\mathrm{LH}}})\left(\frac{1}{T_{\mathrm{surf}}} - \frac{1}{T_E}\right) dA,$$

(13)

basically because we are overestimating the temperature difference across which the irreversible heat transport takes place. See the appendix for a detailed derivation of inequality (13). Note that, as said, vertical fluxes are positive upward. By considering the energy balance at surface, we have that $\overline{F_{z,\mathrm{surf}}^{\mathrm{SW}}} + F_{z,\mathrm{surf}}^{\mathrm{LW}} + \overline{F_{z,\mathrm{surf}}^{\mathrm{SW}}} + F_{z,\mathrm{surf}}^{\mathrm{LH}} = -\mathbf{V_H} \cdot \overline{H_{\mathrm{surf}}}$, where $\mathbf{V_H} \cdot \overline{H_{\mathrm{surf}}}$ is the horizontal divergence of the transport performed by the ocean. By comparing Eqs. (12) and (13), we obtain that the material entropy production by dissipation of kinetic energy is bounded from below by the entropy produced by the large-scale horizontal transport of heat:

$$\int_A \frac{\overline{\varepsilon^2}}{T_{\mathrm{diss}}}\, dA > -\int_A \frac{\mathbf{V_H} \cdot \overline{\mathbf{H}}}{T_E}\, dA$$

$$-\int_A \mathbf{V_H} \cdot \overline{H_{\mathrm{surf}}}\left(\frac{1}{T_{\mathrm{surf}}} - \frac{1}{T_E}\right) dA$$

$$\approx -\int_A \frac{\mathbf{V_H} \cdot \overline{\mathbf{H}}}{T_E}\, dA.$$

(14)

Under the reasonable hypothesis that $(1/T_{\mathrm{surf}} - 1/T_E)$ is approximately constant (roughly corresponding to a spatially homogeneous atmospheric lapse rate), the second term in the first inequality is negligible, since the area integral of the horizontal convergence of subsurface enthalpy flux vanishes. Even with a more conservative scale analysis, we basically obtain the same result, because $|1/T_E| \gg |1/T_{\mathrm{surf}} - 1/T_E| = |1/T_E| \times |(T_E - T_{\mathrm{surf}})/T_{\mathrm{surf}}|$ and in present-day climate the ocean enthalpy transport contributes to about 30% of the total enthalpy transport (Lucarini and Ragone 2011). Equation (14) implies that $\dot{S}_{\mathrm{mat}}^{\mathrm{diss}} > \dot{S}_{\mathrm{mat}}^{\mathrm{hor}}$; that is, the material entropy production by dissipation of kinetic energy is bounded from below by the entropy produced by the horizontal transport of heat performed by the large-scale motion.

Moreover, Eq. (14) allows us to derive an approximate inequality providing a constraint on $\overline{W} = \overline{D} = \int \overline{\varepsilon^2} \, dV$. As half of the kinetic energy is dissipated mainly at the boundary layer and half in the free atmosphere (Peixoto and Oort 1992), we have $T_E \lesssim T_{\text{diss}} \lesssim T_{\text{BL}} \approx T_{\text{surf}}$. Since $\overline{\varepsilon^2}$ is positive definite and the fractional spatial variation of T_S is relatively small, we derive a lower bound $\overline{W}_{\min}$ as

$$
\overline{W} = \overline{D} = \int_A \overline{\varepsilon^2} \, dA \geq -\langle T_{\text{surf}} \rangle \int_A \frac{\mathbf{V_H} \cdot \overline{\mathbf{H}}}{T_E} \, dA
$$
$$
\geq -\langle T_E \rangle \int_A \frac{\mathbf{V_H} \cdot \overline{\mathbf{H}}}{T_E} \, dA = \langle T_E \rangle \overline{\dot{S}^{\text{hor}}_{\text{mat}}} = \overline{W}_{\min}, \quad (15)
$$

where the angle brackets indicate spatial averaging, the second inequality results from $\langle T_{\text{surf}} \rangle \geq \langle T_E \rangle$, and we consider the definition of $\overline{\dot{S}^{\text{hor}}_{\text{mat}}}$ given in Eq. (12). By using $\overline{F^{\text{SW}}_{z,\text{TOA}}} + \overline{F^{\text{LW}}_{z,\text{TOA}}} = -\overline{R} = -\nabla_{\mathbf{H}} \cdot \overline{\mathbf{H}}$, we then express the constraint on the intensity of the Lorenz energy cycle and on the corresponding rate of dissipation of the kinetic energy purely by means of quantities that can be derived from measurements (or model data) evaluated at the top of the atmosphere as follows:

$$
\overline{W}_{\min} = -\langle T_E \rangle \int_A \frac{\overline{R}}{T_E} \, dA. \quad (16)
$$

Note that we have defined the TOA radiation balance $\overline{R}$ as positive (negative) where the system behaves as a net absorber (emitter) of radiation, which is typically the case at low (high) latitudes. It is possible to verify the physical consistency of Eq. (16) considering the following extreme scenario. If the planet has no atmosphere, so that $\overline{W} = 0$, the right term of the inequality must also be vanishing. This is consistent with the fact that in the absence of a fluid envelope, no enthalpy can be transported horizontally, so that when long-term averages are considered, $-\overline{R} = -\nabla_{\mathbf{H}} \cdot \overline{\mathbf{H}} = \overline{F^{\text{SW}}_{z,\text{TOA}}} + \overline{F^{\text{LW}}_{z,\text{TOA}}} = 0$. This implies that the SW and LW fluxes at the top of the (infinitesimal) atmosphere—as well as at surface—have to be everywhere equal in magnitude and opposite in sign.

a. Baroclinic efficiency

We can rewrite Eq. (16) as follows:

$$
\overline{W}_{\min} = -\langle T_E \rangle \left(\int_{A_>} \frac{\overline{R}}{T_E} \, dA + \int_{A_<} \frac{\overline{R}}{T_E} \, dA \right), \quad (17)
$$

where we have divided the domain into two regions $A_>$ and $A_<$, the former (latter) describing the subdomain featuring a positive (negative) radiation budget at the top of the atmosphere. We can express Eq. (17) as

$$
\overline{W}_{\min} = -\langle T_E \rangle \left(\frac{\langle \overline{R} \rangle_> |A_>|}{T_E^>} + \frac{\langle \overline{R} \rangle_< |A_<|}{T_E^<} \right), \quad (18)
$$

where $\langle R \rangle_>$ is the spatial average of the net radiative budget performed on the 2D domain $A_>$ (having measure $|A_>|$), with equivalent notation applying for the negative radiative balance case. Note that $|A_>| + |A_<| = |A|$. Since $\int_A \overline{R} \, d\sigma = 0$, we have that $\langle \overline{R} \rangle_> |A_>| + \langle \overline{R} \rangle_< |A_<| = 0$. Instead, $T_E^>$ and $T_E^<$ are reference temperatures obtained by averaging the emission temperature over the domains $A_<$ and $A_<$, respectively, and, using the value of the net radiative budget as weighting function,

$$
T_E^{>(<)} = \frac{\displaystyle\int_{A_{>(<)}} \overline{R} \, dA}{\displaystyle\int_{A_{>(<)}} (\overline{R}/T_E) \, dA}. \quad (19)
$$

We then obtain

$$
\overline{W}_{\min} = \langle \overline{R} \rangle_> |A_>| \langle T_E \rangle \left(\frac{1}{T_E^<} - \frac{1}{T_E^>} \right) = \eta_h \langle \overline{R} \rangle_> |A_>|, \quad (20)
$$

with

$$
\eta_h = \langle T_E \rangle \left(\frac{1}{T_E^<} - \frac{1}{T_E^>} \right) \approx \frac{T_E^> - T_E^<}{\langle T_E \rangle} \approx \frac{T_E^> - T_E^<}{T_E^>}, \quad (21)
$$

where we have assumed that $\langle T_E \rangle \approx (1/2)(T_E^> + T_E^<)$ and that $(T_E^> - T_E^<)/\langle T_E \rangle \ll 1$. Whereas the first assumption is quite obvious, since we are averaging over two regions $A_>$ and $A_<$ of analogous size, we underline that the second assumption is usually verified even in the presence of large spatial variability of the radiative balance, as a fourth root is involved in the definition of the emission temperature. The quantity η_h links the input of radiative energy at an average rate $\langle \overline{R} \rangle_> |A_>|$ into the warm subdomain at temperature $T_E^>$ to the lower bound to the average rate of production of mechanical work, and can be interpreted as the climate Carnot-like efficiency related *only* to differential heating at the top of the atmosphere.

The overall energy balance of the climate system imposes that the fluid envelope of the planet transports through large-scale motions an amount of enthalpy $\overline{F} = \langle \overline{R} \rangle_> |A_>|$ from the regions of the climate system featuring a positive radiative budget at the top of the atmosphere to those that constantly lose energy to space (Lorenz 1967; Stone 1978a; Peixoto and Oort 1992; Lucarini and Ragone 2011). Because of the fairly zonal

nature of the net TOA radiative balance (Peixoto and Oort 1992), such compensation translates into the fact that in each hemisphere the location of the peak of the meridional enthalpy transport coincides with the latitudinal boundary dividing the radiatively heated low latitudes and the radiatively cooled high latitudes in both the Northern and Southern Hemisphere. Moreover, since the two hemispheres are rather similar in terms of average zonal energy budgets and inferred meridional transports, as imposed by the constraints given in Stone (1978a) and confirmed by Lucarini and Ragone (2011), the intensity of the peak of the transport in either hemisphere is approximately $(1/2)\langle \overline{R}_> \rangle |A_>|$. The lower bound to the intensity of the Lorenz energy cycle given in Eq. (20) can be interpreted as product of an efficiency related to meridional temperature differences and the fluxes across such meridional gradients. This provides further theoretical insight and suitable conceptual framework to the intuition by Barry et al. (2002) as to the possibility of defining a "baroclinic heat engine" extracting work from the meridional heat flux.

What is presented here gives the basic ingredients for providing a rigorous construction of the simplified two-box model usually considered in the literature (Lorenz et al. 2001). Such a reduced model, which allows for the description of entropy production due to horizontal processes of heat exchange only, is enclosed in a dashed rectangle in Fig. 1. The warm box (box 1) is defined by the portion of the fluid envelope of the climate system featuring a positive net radiative balance at TOA and has a temperature equal to $T_E^>$. The cold box (box 2) is defined by the part of the fluid envelope of the planet featuring a negative net radiative balance at TOA (i.e., the middle and high latitudes) and has temperature equal to $T_E^<$. The irreversible heat transfer $\overline{F} = \langle \overline{R} \rangle_> |A_>|$ from warm to cold areas generates entropy at the following rate:

$$\overline{\dot{S}_{mat}^{hor}} = \langle \overline{R} \rangle_> |A_>|(1/T_E^< - 1/T_E^>) = \eta_h \overline{F}/\langle T_E \rangle. \quad (22)$$

b. Bound on the degree of irreversibility of the system

The bound $\overline{\dot{S}_{mat}^{diss}} > \overline{\dot{S}_{mat}^{hor}}$ obtained in Eq. (14) can be used to introduce a further bound to the thermodynamic properties of the system. With a trivial manipulation of the expression of the parameter of irreversibility α, we obtain

$$\alpha = \frac{\overline{\dot{S}_{mat}} - \overline{\dot{S}_{mat}^{diss}}}{\overline{\dot{S}_{mat}^{diss}}} < \frac{\overline{\dot{S}_{mat}} - \overline{\dot{S}_{mat}^{hor}}}{\overline{\dot{S}_{mat}^{diss}}} \approx \frac{\overline{\dot{S}_{mat}^{vert}}}{\overline{\dot{S}_{mat}^{diss}}} = \alpha_{max}, \quad (23)$$

where α_{max} is the upper bound to the parameter of irreversibility. Observing that the Bejan number Be,

a widely used parameter in the applied thermodynamics literature (Paoletti et al. 1989), can be written as Be = $\alpha + 1$, we obtain

$$\frac{\overline{\dot{S}_{mat}}}{\overline{\dot{S}_{mat}^{hor}}} \approx \frac{\alpha_{max} + 1}{\alpha + 1} = \frac{Be_{max}}{Be} \approx \frac{\overline{W}}{\overline{W}_{min}} \quad (24)$$

so that the product of the lower bound to the intensity of the Lorenz energy cycle and of the upper bound of the Bejan number is equal to the product of the actual Bejan number times the actual intensity of the Lorenz energy cycle.

4. Estimation of the thermodynamic properties of PCMDI/CMIP3 climate models

The theory developed in the previous sections is applied to analyze the thermodynamic properties of state-of-the-art CMs using the publicly available output from the PCMDI/CMIP3 dataset (http://www-pcmdi.llnl.gov/). We have used a 100-yr time series of monthly means of radiative fluxes (longwave and shortwave) at the surface and at the top of the atmosphere, from the PI control run scenario. Since for one of these models we have an exact computation of the material entropy production budget in the PI scenario (Pascale et al. 2010), we can also test the accuracy of our approximations in these conditions. The PCMDI/CMIP3 dataset includes data from over 20 CMs, but only 14 CMs were considered in this analysis because of the lack of some fields and/or inconsistencies in the dataset. Models making use of flux adjustments have been excluded too, since they provide an unphysical representation of the thermodynamics of the climate system. [See Table 1 for the list of models used in this paper. Each model is labeled with a number as in Lucarini and Ragone (2011).]

In PI conditions, all the parameters of the model are kept constant (in particular the CO_2 concentration is fixed at 280 ppm), so that the slowest forcing acting on the system is given by the seasonal cycle (the solar cycle, albeit very weak, is considered in some models). Therefore, integrating the model over a sufficiently long time period, the system should reach a stationary state. Once the steady state is reached, the minimal time-averaging window over which one can expect time-independent statistical properties is given by one year. In the following, the time-averaging operator $\overline{(\cdot)}$ used throughout the formulas derived in this paper is considered to act over one year. The consideration of 100 yr for each CM allows the construction of suitable, robust statistics for the yearly averaged thermodynamic properties of the corresponding climate.

TABLE 1. CM numbers as in Lucarini and Ragone (2011) and PI scenario acronyms and expansions used in this study.

CM No.	Acronym	Expansion
1	BCCR BCM2.0	Bjerknes Centre for Climate Research Bergen Climate Model version 2.0
4	CNRM CM3	Centre National de Recherches Météorologiques Coupled Global Climate Model, version 3
6	CSIRO Mk3.5	Commonwealth Scientific and Industrial Research Organisation Mark version 3.0
7	FGOALS	Flexible Global Ocean–Atmosphere–Land System Model
8	GFDL CM2.0	Geophysical Fluid Dynamics Laboratory Climate Model version 2.0
9	GFDL CM2.1	GFDL Climate Model version 2.1
10	GISS AOM	Goddard Institute for Space Studies Atmosphere–Ocean Model
13	HadCM3	Third climate configuration of the Met Office Unified Model
14	HadGEM	Hadley Centre Global Environmental Model
15	INM CM3.0	Institute of Numerical Mathematics Coupled Model, version 3.0
16	IPSL CM4	L'Institut Pierre-Simon Laplace Coupled Model, version 4
17	MIROC3.2(hires)	Model for Interdisciplinary Research on Climate 3.2, high-resolution version
18	MIROC3.2(medres)	Model for Interdisciplinary Research on Climate 3.2, medium-resolution version
20	ECHAM5/MPI OM	ECHAM5/Max Planck Institute Ocean Model

In general, the stationary state of a nonequilibrium system is characterized by vanishing global balances of energy and entropy (Lucarini 2009a) and by time-independent statistical properties for the state variables of the system. While this second condition is fulfilled by the climate models considered here, basically by definition of PI control run, the first condition is, in general, not satisfied, as investigated in Lucarini and Ragone (2011), where significant biases have been found in the global energy balances of the system and of its principal subsystems for these models in PI conditions. Nevertheless, as discussed below, it is still possible to take care of such unphysical biases as done in Lucarini and Ragone (2011) when computing the meridional enthalpy transport.

There are algebraically different ways to define the yearly value of T_E. Since the multiplicative factor to the annual mean of the radiative balance in Eqs. (11) and (12) is $1/T$, we have computed the monthly emission temperatures $T_E^m = \sqrt[4]{F_{z,\text{TOA}}^{\text{LW},m}/\sigma}$, where $F_{z,\text{TOA}}^{\text{LW},m}$ is the monthly mean of the longwave emission at TOA, and than we have computed T_E as the inverse of the annual mean of the inverse of T_E^m:

$$T_E = (\overline{1/T_E^m})^{-1}. \qquad (25)$$

Rather than considering the actual surface temperature fields provided by the CMs, in order to be consistent with the idea of estimating the thermodynamics properties starting from radiative fields only, the considered surface temperature field T_{surf} has been computed from the outgoing longwave radiation at surface by mirroring the procedure described above for computing the 2D T_E starting from the TOA outgoing longwave radiation, thus assuming an unit value for emissivity everywhere and at all times. We have verified that the consideration of the surface temperature fields given as outputs by the CMs impacts our results in an entirely negligible way.

The presence of a spurious bias in the TOA global energy balance has been approximately cured by subtracting at each grid point in each year the globally averaged TOA global energy imbalance. This is a standard procedure when inferring the meridional enthalpy transports, as discussed in Carissimo et al. (1985) and Lucarini and Ragone (2011), and it is justified by the fact that the global energy imbalance at each year is small if compared to the latitudinal variability of the energy balance (on the order of 1 vs 100 W m^{-2}), the quantity in which we are mostly interested. When considering entropy estimators, it is especially important to remove the bias in the TOA energy balance because the related relative error in the estimate of the horizontal component of the material entropy production would be large.

In the case of the net radiative balance at the surface we do not have a zero-sum constraint (latent and sensible heat are not involved in our calculations) because, on the contrary, the typical value of the net global radiative balance at the surface is on the order of 100 W m^{-2}. Thus, it is not possible to define a bias by observing the violation of the zero mean constraint. In any case, even if the bias were on the order of 10 W m^{-2}, the resulting error in estimating the vertical contribution to the material entropy production would be on the order of 5%, so we can safely ignore it.

We have then computed for each model the yearly value of $\dot{S}_{\text{mat}}$, $\dot{S}_{\text{mat}}^{\text{vert}}$, $\dot{S}_{\text{mat}}^{\text{hor}}$, $T_E^<$, $T_E^>$, η_h, and $\overline{W}_{\text{min}}$. From the obtained 100-yr time series we have then estimated the expectation value and the confidence interval of the mean of each quantity using the block-bootstrap resampling technique (see, e.g., Lucarini and Ragone 2011). For all the considered time series the standard deviation is very small, so that the width of the 95% confidence interval is in all cases below 1% of the expectation value. In Table 2 we provide estimates of

TABLE 2. Thermodynamic parameters of PCMDI/CMIP3 CMs in PI conditions.

CM No.–PI scenario	$T_E^>$ (K)	$T_E^<$ (K)	η_h	$\overline{F}/A$ (W m⁻²)	$\overline{W}_{min}/A$ (W m⁻²)	Be$_{max}$	$\overline{\dot{S}_{mat}^{hor}}/A$ (×10⁻³ W m⁻² K⁻¹)	$\overline{\dot{S}_{mat}^{vert}}/A$ (×10⁻³ W m⁻² K⁻¹)	$\overline{\dot{S}_{mat}}/A$ (×10⁻³ W m⁻² K⁻¹)
1–BCCR BCM2.0	241.9	257.6	0.061	20.6	1.25	10.0	5.2	47.2	52.4
4–CNRM CM3	241.5	256.2	0.057	19.2	1.10 3.1[a]	11.7 4.1[b]	4.6	49.2	53.8
6–CSIRO Mk3.5	243.8	254.5	0.042	21.7	0.92	14.5	3.8	51.4	55.2
7 – FGOALS	240.1	256.3	0.063	21.0	1.33	10.2	5.6	52.0	57.6
8–GFDL CM2.0	242.9	257.0	0.055	21.6	1.19	11.3	4.9	50.5	55.4
9–GFDL CM2.1	243.6	258.0	0.056	21.7	1.21	11.2	5.0	51.4	56.4
10–GISS AOM	243.1	257.2	0.055	24.0	1.31	12.1	5.4	60.4	65.8
13–HAD CM3	243.5	259.0	0.060	21.6	1.29 3.1[c]	10.0 4.2[c,d] 4.1[b]	5.3	48.7	54.0
14–HAD GEM	243.4	259.8	0.063	22.6	1.43	9.4	5.9	50.5	56.4
15–INM CM3.0	243.5	255.5	0.047	23.9	1.13	12.7	4.6	53.9	58.5
16–IPSL CM4	243.5	258.1	0.057	24.9	1.41	9.5	5.8	49.5	55.3
17–MIROC3.2 hires	243.4	257.3	0.054	20.5	1.11	12.1	4.5	50.2	54.7
18–MIROC3.2 medres	242.3	255.9	0.053	21.4	1.14 2.7[a]	11.2 4.7[a,d]	4.7	48.4	53.1
20–ECHAM5/MPI OM	242.8	256.8	0.055	24.6	1.34 3.3[a] 2.6[e]	10.4 4.2[a,d] 5.3[d,e]	5.6	53.1	58.7

[a] Actual value of the intensity of the Lorenz energy cycle in twentieth century simulation runs (Marques et al. 2011).

[b] True Bejan number obtained from the entropy production diagnostics reported for the PI simulation run (Pascale et al. 2010).

[c] Actual value of the intensity of the Lorenz energy cycle in the PI simulation run (Pascale et al. 2010).

[d] True Bejan number computed using Eq. (22) in the text using data of $\overline{W}_{min}$, $\overline{W}$, and Be$_{max}$.

[e] Actual value of the intensity of the Lorenz energy cycle in the PI simulation run, but using lower resolution (Hernández-Deckers and von Storch 2010).

the expectation values of the considered thermodynamic parameters.

a. Mean values

The entropy budget of CM 13 has been extensively analyzed in PI conditions in Pascale et al. (2010), so that we have an excellent test for the accuracy of our approximated formulas. Equation (13) gives an estimate for the global material entropy production for CM 13 of 54.0 mW m⁻² K⁻¹, which is in excellent agreement with the correct value of 51.8 mW m⁻² K⁻¹ obtained by Pascale et al. (2010). This single test is highly encouraging in suggesting that our approximate approach provides an accurate guidance and rather stringent estimates of the actual material entropy production of the system, with an uncertainty of about 5%.

For explanatory purposes, in Figs. 2a and 2b we present maps of the average rate of material entropy production by vertical and horizontal processes, respectively, while in Fig. 2c we show the value of T_E. All outputs are obtained from CM 13, even if all CMs give qualitatively similar pictures.

In Fig. 2a we observe that, consistently with the discussion in section 2c, the spatial field whose integral gives $\overline{\dot{S}_{mat}^{vert}}$ is positive everywhere except in small areas at high elevation and latitude where very small negative contributions are obtained. These unphysical results are due to the large temperature inversion observed in these areas, which somewhat compromises the scaling analysis we have adopted. In any case, the global effect of these contributions is entirely negligible. As expected, high values are observed where intense evaporation is present, as in the warm pool of the western Pacific and Indian Ocean, whereas very low values are consistently observed in the cold tongue of the eastern Pacific, near western boundary currents, and in the temperate and cold oceans, while the Mediterranean Sea stands out as a warm pool. Land areas typically feature much lower values than ocean areas at similar latitudes, except for areas characterized by warm and moist climate, such as in the equatorial forests of Amazon, Congo, and Southeast Asia, where water is always available for evaporation and oceanlike values are obtained. The relevance of the vertical latent heat transport in determining the entropy production is also clarified by the fact that values close to zero are found in deserts (e.g., the Sahara, the Kalahari, Central Asia, southwestern United States and Mexico, southern Australia, and Patagonia), even if intense
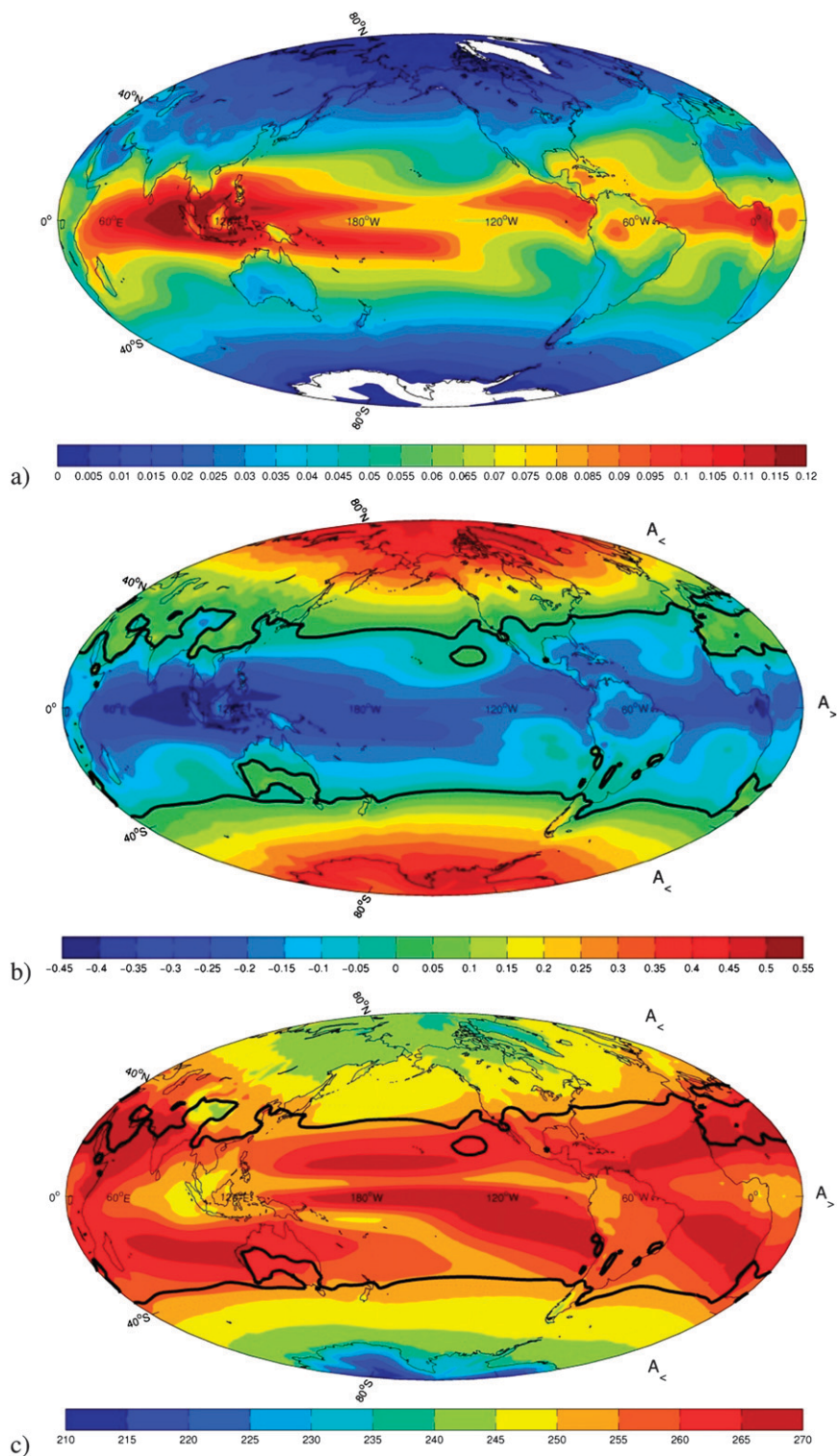
FIG. 2. CM 13's time-averaged spatial fields of (a) $\overline{S}_{mat}^{vert}$ (W m^{-2} K^{-1}), (b) $\overline{S}_{mat}^{hor}$ (W m^{-2} K^{-1}), and (c) T_E (K). In (b) and (c) the solid black line separates $A_>$ and $A_<$.

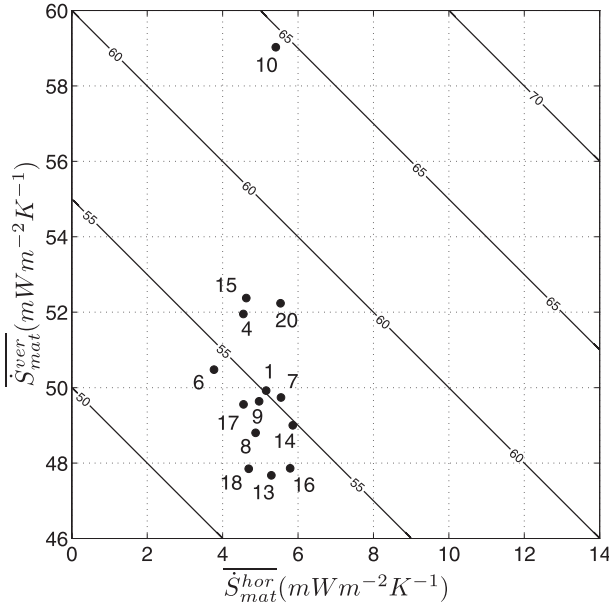FIG. 3. Material entropy production in PCMDI/CMIP3 CMs in PI scenario runs. The contributions due to $\dot{S}_{mat}^{hor}$ and $\dot{S}_{mat}^{vert}$ are depicted. Isolines of the total value of the material entropy production are shown as solid lines.

sensible heat exchanges take place, and in middle and high latitudes of terrestrial areas. At polar latitudes, vanishing values are obtained since convective processes are very weak and moisture is almost absent.

Figure 2b shows that the globally positive value of material entropy production due to horizontal processes results from the (almost perfect; see below) compensation between positive and negative values, with the former dominating the middle and high latitudes and the latter present in the equatorial and tropical regions. Interestingly, some of the features observed in Fig. 2a are found also here: the areas of vigorous moist convection appear as areas of strong negative values related to divergence of (mostly) latent heat. It is also important to note that deserts feature positive values, as they cannot contribute to the latent heat transport and are characterized by high albedo.

Figure 2c shows that, generally, lower (higher) T_E is found in the $A_<$ ($A_>$) area, which clarifies that $T_E^> > T_E^<$ (see below). Nonetheless, local violations to the simple rule "$A_> \rightarrow$ hot and $A_< \rightarrow$ cold" are found. In fact, the intertropical convergence zone (included in $A_>$) features relatively low emission temperatures, since deep convection creates LW radiation-opaque clouds at very high altitude, whereas, over deserts (included in $A_<$) very high emission temperatures are found because of the low cloud coverage.

In Fig. 3 we present a scatterplot of the globally averaged, annual mean values of the vertical and horizontal

components of the material entropy production superimposed on the isolines of its total value. The error bars represent the 95% confidence interval of the estimate and are so small that they are virtually invisible. Models are labeled with numbers as in Table 3. We can see that, apart from CM 10, the typical value of the annual material entropy production is between 52 and 58 mW m^{-2} K^{-1}. These figures match well with the approximate estimate by Ambaum (2010). The contributions to material entropy production due to vertical and horizontal processes typically amount to about 50 and about 5 mW m^{-2} K^{-1}, respectively, so that the contribution due to vertical processes is dominant by about one order of magnitude.

Figure 3 suggests that the anomalously high total material entropy production of CM 10 is due to a large contribution from vertical processes, while the contribution to horizontal component is consistent with the values of the other models. In Lucarini and Ragone (2011), CM 10 was found to be the only model with a negative annual global oceanic energy balance. This suggests that an excess of energy is transported into the atmosphere, mostly due to convective processes, with a resulting positive anomaly in entropy production. This hints at some problems in the representation of convective processes, whose parameterization is especially problematic in a coarse-resolution model such as CM 10. Quite reassuringly, the figure we obtain for the total material entropy production for CM 10 agrees with that found by Goody (2000) in a similar version of the same model.

CM 6 features a small horizontal component of the material entropy production compared to the other models, even if this does not impact substantially the value of the total material entropy production, given the small weight of the contribution of the horizontal processes. In Lucarini and Ragone (2011), CM 6 was found to have the peak of the annual meridional enthalpy transport located anomalously near the equator with respect to the other models (most notably in the Northern Hemisphere). This is consistent with CM 6 having a small material entropy production from horizontal processes, since in this model most of the transport is realized at lower latitudes, where the meridional temperature gradient is smaller.

In Fig. 4 we present a scatterplot of $T_E^<$ and $T_E^>$ together with the corresponding isolines of η_h, which are almost indistinguishable from straight lines. We can see that models feature values of $T_E^<$ between around 240 and 244 K, and values of $T_E^>$ between around 255 and 260 K, so that the typical equivalent temperature difference is about 15 K. Lucarini and Ragone (2011) proposed that spurious positive energy imbalances at steady state due to inconsistencies in the treatment of

TABLE 3. Correlations between thermodynamic parameters of PCMDI/CMIP3 CMs in PI conditions. Statistically significant values are depicted in boldface, where the half-width of the 95% confidence interval is 0.2.

CM No.–PI scenario	$C(\dot{\overline{S}}_{mat}^{hor}, \eta_h)$	$C(\dot{\overline{S}}_{mat}^{hor}, \overline{F})$	$C(\overline{F}, \eta_h)$	$C(\dot{\overline{S}}_{mat}^{hor}, \dot{\overline{S}}_{mat}^{vert})$
1–BCCR BCM2.0	**0.81**	**0.60**	0.02	**0.51**
4–CNRM CM3	**0.86**	**0.19**	−0.34	**0.74**
6–CSIRO Mk3.5	**0.99**	−0.46	−0.59	**0.59**
7–FGOALS	**0.82**	0.38	−0.22	**0.52**
8–GFDL CM2.0	**0.90**	−0.27	−0.65	0.06
9–GFDL CM2.1	**0.70**	0.18	−0.58	0.24
10–GISS AOM	**0.84**	0.04	−0.51	−0.20
13–HAD CM3	**0.78**	**0.53**	−0.13	**0.40**
14–HAD GEM	**0.93**	0.04	−0.34	0.08
15–INM CM3.0	**0.96**	0.36	0.07	**0.55**
16–IPSL CM4	**0.87**	0.18	−0.33	**0.61**
17–MIROC3.2 hires	**0.90**	0.23	−0.23	0.24
18–MIROC3.2 medres	**0.82**	**0.52**	−0.06	**0.56**
20–ECHAM5/MPI OM	**0.88**	0.29	−0.19	**0.69**

energy exchanges throughout the climate system induce the presence of a cold bias when emission temperatures are considered. In agreement with this, in the present analysis we find that the coldest CMs are for the most part those featuring rather large positive global energy imbalances in Lucarini and Ragone (2011), whereas the warmest CMs feature average global energy balances close to zero.

Most models feature values of η_h between 0.050 and 0.060, with a few models in the range of 0.040–0.050 on one side and 0.060–0.065 on the other side. Since CMs differ much more with regard to $T_E^>$ than to $T_E^<$, the largest and smallest efficiencies are related basically to very high and very low values of $T_E^>$, respectively, so that the low latitudes seem to have a prominent role in determining the efficiency of the baroclinic engine. By comparing the figures reported in Table 2 as to the value of $\overline{F} = \langle \overline{R} \rangle_> |A_>|$ and the sum of the peaks of the meridional transports in the Northern and Southern Hemispheres given in Lucarini and Ragone (2011), we find that the meridional heat transport provides for all CMs a contribution of about 95% to the total transport from radiatively warmer to radiatively cooled areas of the climate system (the remaining 5% is due to zonal heat fluxes). Therefore, the interpretation of η_h as the baroclinic efficiency introduced by Barry et al. (2002) is definitely appropriate.

In Table 2 we also provide for all CMs the estimates of the lower bound to the intensity of the Lorenz energy cycle for all considered CMs, computed according to Eq. (16). Most values span the range 1.0–1.5 W m^{-2}, which definitely captures the right order of magnitude of the Lorenz energy cycle (Peixoto and Oort 1992). Fortunately, the scientific literature provides some benchmarks to be used to test how stringent our bounds are. In the case of CM 13, Pascale et al. (2010) report that the

intensity of the Lorenz energy cycle is about 3.1 W m^{-2} in simulations mirroring exactly the PI conditions considered here. This implies that the lower bound underestimates the actual value by 60%. In the case of CM 4, CM 18, and CM 20, Marques et al. (2011) provide estimates for the intensity of the Lorenz energy cycle of 2.7, 3.1, and 3.3 W m^{-2}, respectively, even if the data are referred to twentieth century simulations rather than PI conditions. Nevertheless, since relatively small changes of CO_2 concentration seem to impact only marginally the Lorenz energy cycle (Lucarini et al. 2010b; Hernández-Deckers and von Storch 2010), we conclude that also for these models the lower bound underestimates the actual
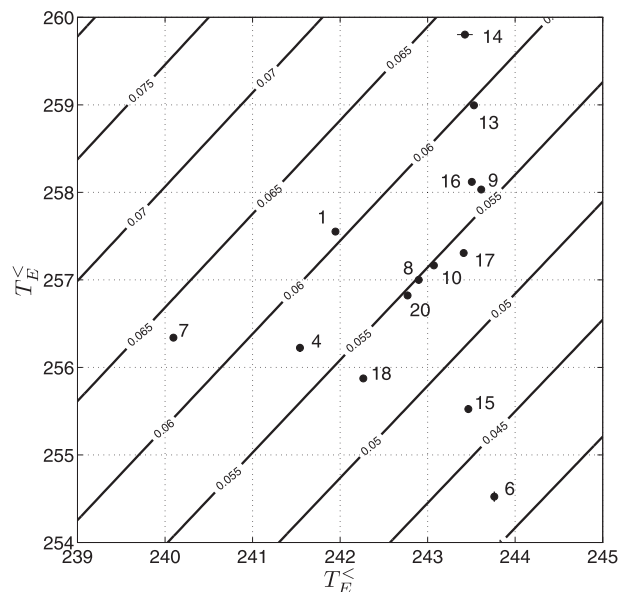

FIG. 4. Equivalent temperatures of the warm $T_E^>$ and cold $T_E^<$ boxes of PCMDI/CMIP3 CMs in PI conditions. Isolines of η_h are indicated with solid lines.
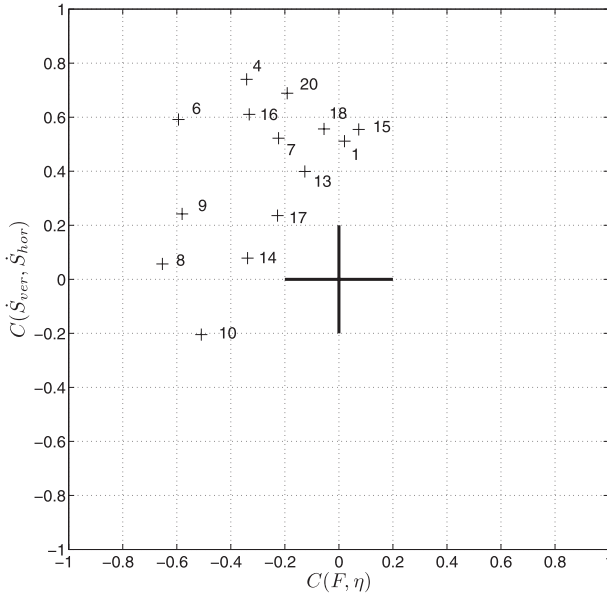
FIG. 5. Strength of the large-scale thermodynamic feedbacks for PCMDI/CMIP3 CMs in PI conditions. Correlation between $\mathbf{F}$ and η_h (x axis) vs correlation between $\dot{S}_{\mathrm{mat}}^{\mathrm{hor}}$ and $\dot{S}_{\mathrm{mat}}^{\mathrm{vert}}$ (y axis).

value by around 60%. These results suggest that our approach is fundamentally correct and the theoretically obtained lower bound provides a good zero-order approximation of the actual value of the intensity of the Lorenz energy cycle.

b. Variability

We now analyze the mutual correlations of the time series of the yearly values of some of the thermodynamic parameters we have derived, in order to improve our understanding of the dynamical processes keeping the system at a well-defined stationary state. Our time series are 100 yr long and feature very weak memory, so that in all cases the 95% confidence interval on the estimates of the correlations has a half-width of 0.2 (see Table 3).

First, we look at potential feedbacks of the system. In Fig. 5 we present a scatterplot of the correlation between the yearly time series of the horizontal baroclinic efficiency η_h and of the total large-scale horizontal transport $\overline{F} = \langle \overline{R} \rangle_{>} A_{>}$ versus the correlation of the yearly time series of the horizontal and vertical contributions to the material entropy production. The uncertainty range of the null hypothesis is represented by the cross centered at (0, 0). We find that nearly all the models feature a statistically significant positive correlation between the horizontal and vertical components of the material entropy production, even if the range of values is quite wide. This implies that there is not such a thing as compensation between the two components, with positive anomalies of one component typically corresponding to negative anomalies of the other

component, thus determining a negative feedback minimizing the variability of the total material entropy production. On the contrary, it is apparent that, when the total material entropy production has, for example, a positive anomaly, both components change accordingly. Figures 2a and 2b are consistent with the idea that the strength of the large-scale tropical convection (which mostly contributes to $\dot{S}_{\mathrm{mat}}^{\mathrm{vert}}$) and of the extratropical dynamics (which mostly contributes to $\dot{S}_{\mathrm{mat}}^{\mathrm{hor}}$) are positively correlated. The positive covariance of the two components of the material entropy production implies that their ratio has a small variability, which, following the discussion presented in section 3b, suggests that the degree of irreversibility is a well-constrained parameters of the system. The only qualitative exception is CM 10, which features a borderline statistically significant negative correlation between the vertical and the horizontal components. Combing this result with the evidence given above on the anomalously high value of material entropy production due to vertical processes (see Fig. 3), we propose that CM 10 might present some issues in the treatment of vertical exchange processes (basically convection) and in their coupling with large-scale processes responsible for horizontal transport.

Looking at the x axis in Fig. 5, we discover that among CMs the values of the correlation between $\overline{F}$ and η_h span a rather wide range, with the majority of models featuring a statistically significant negative correlation. Since the efficiency is a normalized measure of the equivalent temperature difference between the warm and the cold box, it is also an integrated measure of the effective meridional temperature gradient realized at the stationary state. Therefore, the presence of a negative correlation between the efficiency and the meridional total transport suggests that a negative feedback acts to dampen large fluctuations of the meridional temperature gradient, in broad agreement with the baroclinic adjustment theory by Stone (1978b).

Nevertheless, we observe that for several models the coupling between the two main major features involved in the large scale reequilibration process—the heat transport and the temperature gradient—is quite weak. These findings seem to be only partially in agreement with the presence of a feedback keeping $\dot{S}_{\mathrm{mat}}^{\mathrm{hor}}$ near an extremum, as implied in previous investigations of the MEPP hypothesis (Kleidon and Lorenz 2005).

Since the value of $\dot{S}_{\mathrm{mat}}^{\mathrm{hor}}$ is proportional to the product of $\overline{F}$ times the temperature difference between the warm and the cold box [see Eq. (19)], and since the correlation between $\overline{F}$ and η_h is in general not very strong, it seems of relevance to check out which of the two factors $\overline{F}$ and η_h is more strongly correlated to $\dot{S}_{\mathrm{mat}}^{\mathrm{hor}}$. This would help in answering the question as to whether the variability of
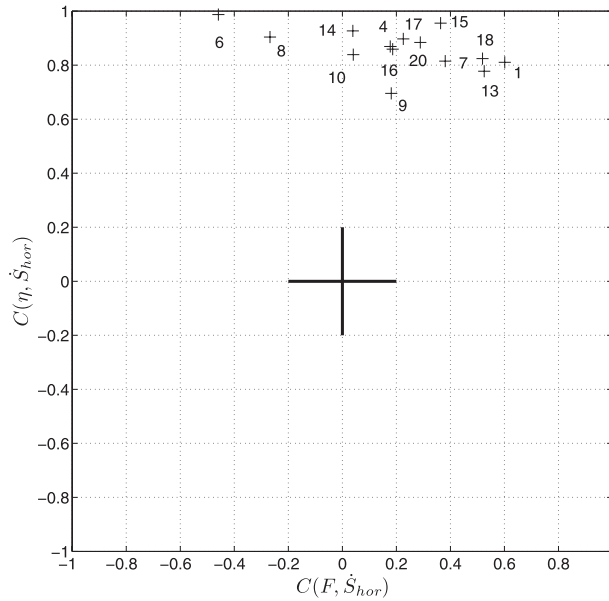
FIG. 6. Correlations between $\overline{\dot{S}_{\mathrm{mat}}^{\mathrm{hor}}}$ and $\overline{F}$ (x axis) and η_h (y axis).

the entropy production is driven more by the temperature differences or by the total heat flux.

In Fig. 6 we see that all CMs feature a very strong positive correlation between the horizontal component of the material entropy production and the efficiency. All values are above 0.7 and several CMs feature correlations above 0.9. Instead, the correlation with the total transport spans over a larger set of values (from -0.5 to 0.6), so that qualitatively different properties are found among CMs. Surprisingly, only a minority of CMs feature a statistically significant positive correlation between $\dot{S}_{\mathrm{mat}}^{\mathrm{hor}}$ and $\overline{F}$. Therefore, the presence of an anomalously high efficiency or, equivalently, of a high equator-to-pole temperature gradient is definitely a better statistical predictor of high entropy production due to horizontal processes. This result suggests that simplified parameterizations of entropy production could be written efficiently in the form $\dot{S}_{\mathrm{mat}}^{\mathrm{hor}} = \dot{S}_{\mathrm{mat}}^{\mathrm{hor}}(\eta_h)$, which provides further evidence of the relevance of the efficiency parameter introduced here.

These results definitely suggest that, as opposed to the climatological averages considered above, CMs are much less consistent with each other in the representation of the second moments of the large-scale thermodynamic properties. This hints at the need for further explorations of the related climate feedbacks.

5. Conclusions

In this paper we have performed a reexamination of material entropy production in the climate system by proposing theoretical advances and by presenting new results derived from control runs of state-of-the-art CMs.

We have first discussed various approaches recently presented in the literature for analyzing the entropy budget in the climate system and concluded, from the critical appraisal of the results presented by Pascale et al. (2010), that the approach of considering a simplified description of a moist atmosphere, where water is treated mainly as a passive substance that provides/removes latent heat, is well suitable when studying the material entropy production.

We have introduced an approximate splitting between material entropy production contributions due to vertical processes, mostly related to convection and characterized by short time scales, and those eminently due to horizontal processes, mostly related to the large-scale motions in the climate system and characterized by longer time scales. Notably, such an approach allows for computing with good precision the material entropy production of the climate system using only 2D radiative fields at the top of the atmosphere and at surface (even if the evaluation of the latter can be experimentally challenging). By comparing our approximate formulas results with the ''quasi-exact'' treatment by Pascale et al. (2010), we find that our 2D simplified calculations are correct to within 5%.

We have derived bounds to basic thermodynamic properties of the climate system based on time-averaged TOA radiative data only. This could in principle be particularly promising especially when one deals with planetary objects, such as distant extrasolar planets, where the amount of observational data is limited. We have proved that the material entropy produced by the horizontal large-scale enthalpy transports is a lower bound to the total material entropy production and, in particular, to its portion related to the dissipation of mechanical energy. From this, a lower bound is derived for the average rate of the Lorenz energy cycle. The Lorenz energy cycle results to be larger than the product of the net input of radiative energy in the positive energy balance regions times a suitably defined baroclinic efficiency, proportional to the difference between the average emission temperatures of areas of the planet with positive and negative radiative balance at the top of the atmosphere. This provides a generalization of the idea that the atmospheric circulation can be described as resulting from a baroclinic heat engine extracting work from the meridional heat flux (Barry et al. 2002). As the meridional heat flux by atmospheric eddies contributes substantially to the total meridional heat flux and, at the same time, plays a fundamental role in the Lorenz energy cycle by transforming zonal into eddy available

potential energy, the presence of such constraints is not so surprising.

We have clarified the relevance of two-box models representative of planetary circulations discussed in, for example, Lorenz et al. (2001). These models, by neglecting vertical processes (which, in the case of our planet, give the dominant contribution to the material entropy production), cannot provide a plausible description of the material entropy production of the climate system, nor can they be used to test MEPP. Instead, a minimal model of material entropy production in a planetary system (schematically depicted in Fig. 1) requires at least four boxes, representing cold and warm pools of fluid and cold and warm surfaces beneath, taking care to represent both horizontal and vertical transport processes.

The evaluation of the contributions to the material entropy production due to horizontal and vertical processes on state-of-the-art CM runs provides rather interesting insights. We discover that models agree within about 10% on the value of total material entropy production; specifically, the disagreements are within about 10% on the value of the vertical term, which is the largely dominant one, whereas larger disagreements (on the order of 20%) exist on the horizontal term, which is about one order of magnitude smaller. Two models seem to be somewhat out of this picture.

Because the entropy production due to horizontal processes can be interpreted as resulting from the large-scale heat transport from low- (warm) to high-latitude (cold) regions, its intensity depends at first order on the product between the maximum intensity of the meridional transport times the differences between the emission temperature of the two regions. Obvious physical balances would suggest that the two factors should be, modelwise, negatively correlated, so that one expects that the agreement among CMs should be better for the entropy production than for the transport diagnostics. Instead, in Lucarini and Ragone (2011) it is shown that discrepancies on the total (and atmospheric) meridional transports among models are also around 20%—it could be argued that a role is played by disagreements on their meridional gradients of albedo [see Probst et al. (2010) for a related analysis on total cloud cover]. As a result, the baroclinic efficiency of the models disagrees substantially, as do the lower bounds to the intensity of the Lorenz energy cycle. For the CMs where independent data on the intensity if the Lorenz energy cycle are available, we find that such bounds are relatively stringent (within a factor of about 2), which supports the relevance of our theoretical results.

We have then explored the second moments of the thermodynamic parameters discussed above by looking at the properties of their correlations, in order to grasp some understanding of the large feedbacks acting on the system. We discover that CMs disagree quantitatively to a much greater extent than when looking at first moments of the considered thermodynamic parameters. Nevertheless, a robust feature of most models is the positive correlation of the contributions to material entropy production due to vertical and horizontal processes. The dynamical link between the tropical and the extratropical dynamics suggests that no compensation mechanism is in place to *control* the total material entropy production. Similarly, most models feature a negative correlation between the intensity of the large-scale heat transport and the difference between the effective emission temperatures of the radiatively heated and cooled areas of the planet, in broad agreement with the theory of baroclinic adjustment. Finally, we discover that such temperature difference (or, equivalently, the baroclinic efficiency of the system) is a much stronger proxy for the material entropy production due to horizontal processes than the heat flux, thus suggesting its great relevance as a large-scale indicator of the climate system.

Future investigations will move along the following lines. First, it is of great interest to study how the increase of greenhouse gases impacts the details of the material entropy production on earth by taking advantage of the PCMDI/CMIP3 dataset. While we expect an overall positive sensitivity of such a thermodynamic parameter—see Lucarini et al. (2010b)—it will be interesting to analyze how climate change effects the contributions to material entropy production due to vertical and horizontal processes. Preliminary analyses on the Special Report on Emissions Scenarios (SRES) A1B scenario runs suggest that the impact has opposite sign for the two terms, with an increase in entropy production due to vertical processes occurring in all CM as a result of enhanced convection. This result, which is apparently at odds with the positive covariability of the annual time series described above in the PI run, casts further doubts in the straightforward applicability of the properties of the natural variability of the climate system properties for inferring the properties of long-term, forced climate variations (Lucarini 2008b, 2009b). As suggested by the maps showing the spatial properties of the thermodynamic fields, the theory presented in this paper can be used also for devising diagnostic tools to be used to analyze local processes and specific geographical features of the climate, both using satellite data and numerical model data. Nonetheless, this requires reexamining in more quantitative terms the scale analysis discussed in this paper and assessing its limitations.

Second, a detailed examination of the Lorenz energy cycle and entropy production of other celestial objects of the solar system seems of great relevance for its own sake,

thus extending the work by Aoki (1983), and for understanding the relevance of the thermodynamic bounds proposed here. It is encouraging to note that various models belonging to the PLASIM family (Fraedrich et al. 2005) have already been adapted to study the atmospheres of Titan (Grieger et al. 2004) and Mars (Stenzel et al. 2007), thus allowing for an integration of satellite and model data. Moreover, observations are providing a growing amount of information on extrasolar planets, whose investigation provides an exciting scientific challenge. Obviously, as the chemical composition, the characteristic temperatures of the atmospheres of planets, and their astronomical parameters exhibit a great variety, the scaling analyses presented here should be carefully reconsidered.

Third, it would be important to reconcile the definition of thermodynamic efficiency proposed by Johnson (2000) and Lucarini (2009a) with that proposed by Ambaum (2010). In this direction, concepts borrowed from endoreversible thermodynamics (Hoffmann et al. 1997) could be of great help.

APPENDIX

Derivation of a Thermodynamic Inequality

In the following we derive the inequality given in Eq. (13), which has served as a starting point for obtaining the lower bounds to the entropy production due to the dissipative processes and to the intensity of the Lorenz energy cycle. In section 2 we have shown that the global material entropy production of the earth system at the steady state can be written as

$$\overline{\dot{S}_{\text{mat}}} = \int_A \frac{\langle \overline{\varepsilon^2} \rangle}{T_{\text{diss}}} dA - \int_A \overline{F_{z,\text{surf}}^{\text{SH}}} \left(\frac{1}{T_{\text{SH}}^+} - \frac{1}{T_{\text{SH}}^-} \right) dA$$
$$- \int_A \overline{F_{z,\text{surf}}^{\text{LH}}} \left(\frac{1}{T_{\text{LH}}^+} - \frac{1}{T_{\text{LH}}^-} \right) dA + \Delta \overline{\dot{S}_{\text{mat}}^{\text{LH}}}, \quad \text{(A1)}$$

where we recall that $\langle \overline{\varepsilon^2} \rangle$ is the vertically integrated dissipational heating (positive definite), $\overline{F_{z,\text{surf}}^{\text{SH}}}$ and $\overline{F_{z,\text{surf}}^{\text{LH}}}$

are the vertical components of the sensible and latent heat fluxes at the surface (positive upward), T_{diss} is the characteristic temperature at which the dissipational heating occurs, T_{SH}^+ and T_{LH}^+ are the characteristic temperatures at which sensible and latent heat are extracted, T_{SH}^- and T_{LH}^- are the characteristic temperature at which sensible and latent heat are absorbed, and $\Delta \overline{\dot{S}_{\text{mat}}^{\text{LH}}}$ represents the correction related to the horizontal transport of water vapor. Defining

$$\Delta \overline{\dot{S}_{\text{mat}}^{\text{corr}}} = -\int_A \overline{F_{z,\text{surf}}^{\text{SH}}} \left(\frac{1}{T_{\text{SH}}^+} - \frac{1}{T_{\text{SH}}^-} + \frac{1}{T_E} - \frac{1}{T_{\text{surf}}} \right) dA$$
$$- \int_A \overline{F_{z,\text{surf}}^{\text{LH}}} \left(\frac{1}{T_{\text{LH}}^+} - \frac{1}{T_{\text{LH}}^-} + \frac{1}{T_E} - \frac{1}{T_{\text{surf}}} \right) dA, \quad \text{(A2)}$$

we can rewrite Eq. (A1) as

$$\overline{\dot{S}_{\text{mat}}} = \int_A \frac{\langle \overline{\varepsilon^2} \rangle}{T_{\text{diss}}} dA - \int_A (\overline{F_{z,\text{surf}}^{\text{SH}}} + \overline{F_{z,\text{surf}}^{\text{LH}}}) \left(\frac{1}{T_{\text{surf}}} - \frac{1}{T_E} \right) dA$$
$$+ \Delta \overline{\dot{S}_{\text{mat}}^{\text{corr}}} + \Delta \overline{\dot{S}_{\text{mat}}^{\text{LH}}}. \quad \text{(A3)}$$

Performing a scale analysis we can compare the relative magnitude and the sign of $\Delta \overline{\dot{S}_{\text{mat}}^{\text{corr}}}$ and $\Delta \overline{\dot{S}_{\text{mat}}^{\text{LH}}}$ in order to understand which is the relation between $\overline{\dot{S}_{\text{mat}}}$ and the first two terms on the rhs of Eq. (A3).

To estimate $\Delta \overline{\dot{S}_{\text{mat}}^{\text{corr}}}$ we make the following assumptions:

- both sensible and latent heat are extracted at surface temperature $T_{\text{SH}}^+ = T_{\text{LH}}^+ = T_{\text{surf}}$;
- the turbulent transport of sensible heat is basically a local process, taking place mostly in the boundary layer, so that $T_{\text{SH}}^- = T_{\text{BL}} > T_E$; and
- the water vapor saturation mixing ratio strongly increases with temperature, and on earth the atmospheric temperature decreases with height. Therefore the vertical scale of water vapor in globally saturated conditions is smaller than that of the atmosphere, and we have that the latent heat is absorbed by the atmosphere at a condensation temperature $T_{\text{LH}}^- = T_C > T_E$.

Thus we have

$$\Delta \overline{\dot{S}_{\text{mat}}^{\text{corr}}} = -\int_A \overline{F_{z,\text{surf}}^{\text{SH}}} \left(\frac{1}{T_E} - \frac{1}{T_{\text{BL}}} \right) dA$$
$$- \int_A \overline{F_{z,\text{surf}}^{\text{LH}}} \left(\frac{1}{T_E} - \frac{1}{T_C} \right) dA < 0 \quad \text{(A4)}$$

because both integrals in Eq. (A4) are positive (remember that the vertical fluxes are positive upward). We can estimate the absolute value of $\Delta \overline{\dot{S}_{\text{mat}}^{\text{corr}}}$ using the following characteristic scale values:

$$T_{\mathrm{BL}} \approx 280\,\mathrm{K}, \quad T_C \approx 260\,\mathrm{K}, \quad T_E \approx 250\,\mathrm{K},$$

$$|\overline{F_{z,\mathrm{surf}}^{\mathrm{SH}}}| \approx 20\,\mathrm{W\,m}^{-2}, \quad \text{and} \quad |\overline{F_{z,\mathrm{surf}}^{\mathrm{LH}}}| \approx 80\,\mathrm{W\,m}^{-2}$$

We obtain

$$|\Delta \overline{\dot{S}_{\mathrm{mat}}^{\mathrm{corr}}}| \approx |\overline{F_{z,\mathrm{surf}}^{\mathrm{SH}}}| \frac{|T_{\mathrm{BL}} - T_E|}{|T_{\mathrm{BL}}||T_E|} + |\overline{F_{z,\mathrm{surf}}^{\mathrm{LH}}}| \frac{|T_C - T_E|}{|T_C||T_E|}$$

$$\approx 20 \times 10^{-3}\ \mathrm{W\,m}^{-2}\,\mathrm{K}^{-1}. \tag{A5}$$

In section 2 we have seen that

$$\Delta \overline{\dot{S}_{\mathrm{mat}}^{\mathrm{LH}}} = -\int_A \overline{F_{\mathrm{out}}^{\mathrm{LH}}} \left(\frac{1}{T_C} - \frac{1}{T_C'} \right) dA, \tag{A6}$$

where $\overline{F_{\mathrm{out}}^{\mathrm{LH}}}$ is the amount of latent heat extracted in a certain atmospheric column that is not absorbed in the same column, T_C is the characteristic temperature of absorption of latent heat as above, and T_C' is the effective temperature at which $\overline{F_{\mathrm{out}}^{\mathrm{LH}}}$ is absorbed (see discussion in section 2). We can give the absolute value of this correction an upper bound as follows:

$$|\Delta \overline{\dot{S}_{\mathrm{mat}}^{\mathrm{LH}}}| < |\overline{F_{\mathrm{max}}^{\mathrm{LH}}}| \frac{|\Delta^{\mathrm{hor}} T_C|}{|T_C|^2} < 5 \times 10^{-3}\ \mathrm{W\,m}^{-2}\,\mathrm{K}^{-1}, \tag{A7}$$

where $|\overline{F_{\mathrm{max}}^{\mathrm{LH}}}| \approx 10$ W m^{-2} is the annual mean of the net transport of latent heat divided by the area of the earth (Peixoto and Oort 1992), $|\Delta^{\mathrm{hor}} T_C| \approx 30$ K is a "generous" measure of the difference of the middle atmospheric temperature between the areas of the planet where the moisture is diverging and converging, and $T_C \approx 260$ K. We note that in this estimate we have considered that all the moisture that is not condensed in the same column where it is evaporated is condensed at a lower (or higher) condensation temperature. On the earth, part of the moisture that evaporates in the tropics is transported and condensed at the equator at a higher condensation temperature (negative contribution to $\Delta \dot{S}_{\mathrm{mat}}^{\mathrm{LH}}$), while part is condensed at the midlatitudes at a lower condensation temperature (positive contribution to $\Delta \dot{S}_{\mathrm{mat}}^{\mathrm{LH}}$), so that the resulting partial compensation ensures us that the obtained bound is even safer. The sign of $\Delta \dot{S}_{\mathrm{mat}}^{\mathrm{LH}}$ depends on which of the two cases gives the dominant contribution.

With this analysis we have that $\Delta \overline{\dot{S}_{\mathrm{mat}}^{\mathrm{corr}}}$ is negative and in absolute value much larger than the upper bound of $\Delta \dot{S}_{\mathrm{mat}}^{\mathrm{LH}}$. Therefore $\Delta \overline{\dot{S}_{\mathrm{mat}}^{\mathrm{corr}}} + \Delta \dot{S}_{\mathrm{mat}}^{\mathrm{LH}} < 0$ and we deduce

$$\overline{\dot{S}_{\mathrm{mat}}} < \int_A \frac{\langle \overline{\varepsilon^2} \rangle}{T_{\mathrm{diss}}} dA - \int_A (\overline{F_{z,\mathrm{surf}}^{\mathrm{SH}}} + \overline{F_{z,\mathrm{surf}}^{\mathrm{LH}}}) \left(\frac{1}{T_S} - \frac{1}{T_E} \right) dA. \tag{A8}$$

REFERENCES

Ambaum, M. H. P., 2010: *Thermal Physics of the Atmosphere.* Wiley, 256 pp.

Aoki, I., 1983: Entropy productions on the earth and other planets of the solar system. *J. Phys. Soc. Japan,* **52,** 1075–1078.

Barry, L., G. C. Craig, and J. Thuburn, 2002: Poleward heat transport by the atmospheric heat engine. *Nature,* **415,** 774–777.

Carissimo, B. C., A. H. Oort, and T. H. Vonder Harr, 1985: Estimating the meridional transports of the atmosphere and ocean. *J. Phys. Oceanogr.,* **15,** 82–91.

de Groot, S., and P. Mazur, 1984: *Non-Equilibrium Thermodynamics.* Dover, 510 pp.

Dewar, R. C., 2005: Maximum entropy production and the fluctuation theorem. *J. Phys.,* **38A,** L371, doi:10.1088/0305-4470/38/21/L01.

Emanuel, K. A., 2000: Quasi-equilibrium thinking. *General Circulation Model Development: Past, Present, and Future,* D. A. Randall, Ed., Academic Press, 225–255.

Fraedrich, K., and F. Lunkeit, 2008: Diagnosing the entropy budget of a climate model. *Tellus,* **60A,** 921–931.

——, H. Jansen, E. Kirk, U. Luksch, and F. Lunkeit, 2005: The planet simulator: Towards a user friendly model. *Meteor. Z.,* **14,** 299–304.

Goody, R., 2000: Sources and sinks of climate entropy. *Quart. J. Roy. Meteor. Soc.,* **126,** 1953–1970.

——, 2007: Maximum entropy production in climate theory. *J. Atmos. Sci.,* **64,** 2735–2739.

Grassl, H., 1981: The climate at maximum entropy production by meridional atmospheric and oceanic heat fluxes. *Quart. J. Roy. Meteor. Soc.,* **107,** 153–166.

Green, J., 1967: Division of radiative streams into internal transfer and cooling to space. *Quart. J. Roy. Meteor. Soc.,* **93,** 371–372.

Grieger, B., J. Segschenider, H. U. Keller, A. V. Rodin, F. Lunkeit, E. Kirk, and K. Fraedrich, 2004: Simulating Titan's tropospheric circulation with the Portable University Model of the Atmosphere. *Adv. Space Res.,* **34,** 1650–1654.

Grinstein, G., and R. Linsker, 2007: Comments on a derivation and application of the "maximum entropy production" principle. *J. Phys.,* **40A,** 9717, doi:10.1088/1751-8113/40/31/N01.

Held, I. M., 2005: The gap between simulation and understanding in climate modeling. *Bull. Amer. Meteor. Soc.,* **86,** 1609–1614.

Hernández-Deckers, D., and J.-S. von Storch, 2010: Energetics responses to increases in greenhouse gas concentration. *J. Climate,* **23,** 3874–3887.

Hoffmann, K. H., J. M. Burzler, and S. Schubert, 1997: Endoreversible thermodynamics. *J. Non-Equilib. Thermodyn.,* **22,** 311–355.

Johnson, D. R., 2000: Entropy, the Lorenz energy cycle, and climate. *General Circulation Model Development: Past, Present, and Future,* D. A. Randall, Ed., Academic Press, 659–720.

Kiehl, J. T., and K. E. Trenberth, 1997: Earth's annual global mean energy budget. *Bull. Amer. Meteor. Soc.,* **78,** 197–208.

Kleidon, A., 2009: Nonequilibrium thermodynamics and maximum entropy production in the earth system. *Naturwissenschaften,* **96,** 655–677.

——, and R. D. Lorenz, Eds., 2005: *Non-Equilibrium Thermodynamics and the Production of Entropy: Life, Earth, and Beyond.* Springer, 260 pp.

——, K. Fraedrich, E. Kirk, and F. Lunkeit, 2006: Maximum entropy production and the strength of boundary layer exchange

in an atmospheric general circulation model. *Geophys. Res. Lett.,* **33,** L06706, doi:10.1029/2005GL025373.

Lorenz, E. N., 1955: Available potential energy and the maintenance of the general circulation. *Tellus,* **7,** 157–167.

——, 1967: *The Nature and Theory of the General Circulation of the Atmosphere.* World Meteorological Organization, 161 pp.

Lorenz, R. D., and N. O. Rennó, 2002: Work output of planetary atmospheric engines: Dissipation in clouds and rain. *Geophys. Res. Lett.,* **29,** 1023, doi:10.1029/2001GL013771.

——, J. I. Lunine, P. G. Withers, and C. McKay, 2001: Titan, Mars, and Earth: Entropy production by latitudinal heat transport. *Geophys. Res. Lett.,* **28,** 415–418.

Lucarini, V., 2008a: Validation of climate models. *Encyclopedia of Global Warming and Climate Change,* G. Philander, Ed., SAGE, 1053–1057.

——, 2008b: Response theory for equilibrium and non-equilibrium statistical mechanics: Causality and generalized Kramers–Kronig relations. *J. Stat. Phys.,* **131,** 543–558.

——, 2009a: Thermodynamic efficiency and entropy production in the climate system. *Phys. Rev. E,* **80,** 021118, doi:10.1103/PhysRevE.80.021118.

——, 2009b: Evidence of dispersion relations for the nonlinear response of the Lorenz 63 system. *J. Stat. Phys.,* **134,** 381–400.

——, and F. Ragone, 2011: Energetics of climate models: Net energy balance and meridional enthalpy transport. *Rev. Geophys.,* **49,** RG1001, doi:10.1029/2009RG000323.

——, K. Fraedrich, and F. Lunkeit, 2010a: Thermodynamic analysis of snowball earth hysteresis experiment: Efficiency, entropy production, and irreversibility. *Quart. J. Roy. Meteor. Soc.,* **136,** 2–11.

——, ——, and ——, 2010b: Thermodynamics of climate change: Generalized sensitivities. *Atmos. Chem. Phys.,* **10,** 3699–3715.

Marques, C. A. F., A. Rocha, and J. Corte-Real, 2011: Global diagnostic energetics of five state-of-the-art climate models. *Climate Dyn.,* **36,** 1767–1794, doi:10.1007/s00382-010-0828-9.

Martyushev, L. M., and V. D. Seleznev, 2006: Maximum entropy production principle in physics, chemistry and biology. *Phys. Rep.,* **426,** 1–45.

Mobbs, S. D., 1982: Extremal principles for global climate models. *Quart. J. Roy. Meteor. Soc.,* **108,** 535–550.

Ozawa, H., A. Ohmura, R. D. Lorenz, and T. Pujol, 2003: The second law of thermodynamics and the global climate system: A review of the maximum entropy production principle. *Rev. Geophys.,* **41,** 1018, doi:10.1029/2002RG000113.

Paltridge, G. W., 1975: Global dynamics and climate—A system of minimum entropy exchange. *Quart. J. Roy. Meteor. Soc.,* **101,** 475–484.

Paoletti, S., F. Rispoli, and E. Sciubba, 1989: Calculation of exergetic losses in compact heat exchanger passages. *ASME AES,* **10,** 21–29.

Pascale, S., J. M. Gregory, M. Ambaum, and R. Tailleux, 2010: Climate entropy budget of the HadCM3 atmosphere–ocean general circulation model and of FAMOUS, its low-resolution version. *Climate Dyn.,* **36,** 1189–1206, doi:10.1007/s00382-009-0718-1.

Pauluis, O., 2000: Entropy budget of an atmosphere in radiative–convective equilibrium. Ph.D. thesis, Princeton University, 274 pp.

——, and I. M. Held, 2002a: Entropy budget of an atmosphere in radiative–convective equilibrium. Part I: Maximum work and frictional dissipation. *J. Atmos. Sci.,* **59,** 125–139.

——, and ——, 2002b: Entropy budget of an atmosphere in radiative–convective equilibrium. Part II: Latent heat transport and moist processes. *J. Atmos. Sci.,* **59,** 140–149.

——, V. Balaji, and I. M. Held, 2000: Frictional dissipation in a precipitating atmosphere. *J. Atmos. Sci.,* **57,** 989–994.

Peixoto, J. P., and A. H. Oort, 1992: *Physics of Climate.* Springer, 520 pp.

——, ——, M. de Almeida, and A. Tome, 1991: Entropy budget of the atmosphere. *J. Geophys. Res.,* **96,** 10 981–10 988.

Prigogine, I., 1962: *Non-Equilibrium Statistical Mechanics.* Wiley, 319 pp.

Probst, P., R. Rizzi, E. Tosi, V. Lucarini, and T. Maestri, 2010: Total cloud cover from satellite observations and climate models. *Atmos. Chem. Phys. Discuss.,* **10,** 21 023–21 046.

Rennó, N. O., 2001: Comments on "Frictional dissipation in a precipitating atmosphere." *J. Atmos. Sci.,* **58,** 1173–1177.

Romps, D. M., 2008: The dry-entropy budget of a moist atmosphere. *J. Atmos. Sci.,* **65,** 3779–3799.

Saltzman, B., 2002: *Dynamical Paleoclimatology: Generalized Theory of Global Climate Change.* Academic Press, 354 pp.

Shimokawa, S., and H. Ozawa, 2001: On thermodynamics of the oceanic general circulation: Entropy increase rate of an open dissipative system and its surroundings. *Tellus,* **53A,** 266–277.

Solomon, S., D. Qin, M. Manning, M. Marquis, K. Averyt, M. M. B. Tignor, H. L. Miller Jr., and Z. Chen, Eds., 2007: *Climate Change 2007: The Physical Science Basis.* Cambridge University Press, 996 pp.

Stenzel, O. J., B. Grieger, H. U. Keller, K. Fraedrich, E. Kirk, and F. Lunkeit, 2007: Coupling Planet Simulator Mars, a general circulation model of the Martian atmosphere, to the ice sheet model SICOPOLIS. *Planet. Space Sci.,* **55,** 2087–2096.

Stone, P. H., 1978a: Constraints on dynamical transports of energy on a spherical planet. *Dyn. Atmos. Oceans,* **2,** 123–139.

——, 1978b: Baroclinic adjustment. *J. Atmos. Sci.,* **35,** 561–571.

Tailleux, R., 2009: On the energetics of stratified turbulent mixing, irreversible thermodynamics, Boussinesq models, and the ocean heat engine controversy. *J. Fluid Mech.,* **638,** 339–382.

Wu, W., and Y. Liu, 2009: Radiation entropy flux and entropy production of the earth system. *Rev. Geophys.,* **48,** RG2003, doi:10.1029/2008RG000275.